

**MONITORING SEATED POSTURAL RESPONSES
TO ASSESS COGNITIVE STATE**

by

Gregory Richard Frank

BS, University of Pittsburgh, 2003

Submitted to the Graduate Faculty of
School of Engineering in partial fulfillment
of the requirements for the degree of
Master of Science

University of Pittsburgh

2006

UNIVERSITY OF PITTSBURGH

SCHOOL OF ENGINEERING

This thesis was presented

by

Gregory Richard Frank

It was defended on

September 22, 2006

and approved by

Donald H. McBurney, Professor Emeritus, Department of Psychology

Mark S. Redfern, Professor, Department of Bioengineering

Thesis Advisor: Carey D. Balaban, Professor, Department of Bioengineering

Copyright © by Gregory Richard Frank

2006

MONITORING OF SEATED POSTURAL RESPONSES

TO ASSESS COGNITIVE STATE

Gregory Richard Frank, M.S.

University of Pittsburgh, 2006

With recent advances in workstation technology, operators are often asked to perform complex tasks that require a tremendous amount of real-time information processing. In order to avoid poor task performance due to the operator's cognitive limitations, it would be advantageous to be able to probe an operator's cognitive state while performing such tasks. The current study investigates whether operators exhibit changes in seated posture as a result of changing cognitive task conditions. Furthermore, the current study presents means of quantifying such seated postural changes in real-time and uses these measures to construct an implicit cognitive state gauge.

Fourteen subjects performed a simulated air space monitoring task in which they tracked multiple 75.0 sec long waves of incoming aircraft with various levels of difficulty. Subjects were instructed to identify all incoming aircraft and to attend to them based on the level of threat that they posed. While performing the task, subjects' seated postural changes were monitored by tracking the distribution of pressure over the seat and back pads of the chair. This distribution of pressure was used to calculate changes in seated center of pressure, seat torsion, and the extent to which subjects used the back of the chair to brace themselves.

Subjects demonstrated a significant decrease in seated postural changes over the course of more difficult waves (high number of aircraft on screen) in comparison to easier waves (low number of aircraft on screen). When subjects completed waves with 24 tracks on screen

compared to waves with 6 tracks on screen, the distance traveled by the seated center of pressure decreased 40.3%, transverse-plane seat torsion decreased 32.2%, and the total change in distance between the left and right ischial tuberosities decreased 38.1% on average. The correlation of subjects' postural changes to the changing number of tracks on screen was consistently high while the number of tracks on screen was increasing and was consistently low after the maximum number of tracks on screen had been presented. It was concluded that specific changes in seated posture can be associated with how subjects update their situational awareness of task conditions.

TABLE OF CONTENTS

NOMENCLATURE.....	XIV
1.0 SPECIFIC AIMS.....	1
2.0 BACKGROUND AND SIGNIFICANCE	3
2.1 SCOPE OF THE PROBLEM.....	3
2.2 RESEARCH BACKGROUND.....	4
2.2.1 Cognition and Task Performance.....	4
2.2.2 Current Gauges of Cognition.....	6
2.2.3 Cognition and Standing Posture.....	9
2.2.4 Cognition and Seated Posture.....	14
2.2.4.1 Nonverbal Communication.....	14
2.2.4.2 Small-Scale Changes in Seated Posture	18
3.0 METHODS	19
3.1 SUBJECT POPULATION.....	19
3.2 EXPERIMENTAL DESIGN	20
3.2.1 Cognitive Task.....	20
3.2.1.1 Warship Commander Protocol	20
3.2.1.2 Trial Sequence.....	23
3.2.2 Experimental Equipment and Environment.....	25
3.2.2.1 Postural Assessment Hardware.....	25
3.2.2.2 Computers	27
3.2.2.3 Workstation Environment	28
3.3 DATA ANALYSIS.....	29
3.3.1 Data Conditioning.....	29
3.3.2 Raw Posture Variables	30
3.3.3 Gross Postural Changes	35

3.3.4	Level of Engagement.....	36
3.3.4.1	Posture-Task Correlation	36
3.3.4.2	Multivariate Discriminant Analysis.....	38
3.3.4.3	Principal Component Analysis	43
3.3.5	Statistical Analysis	46
4.0	RESULTS	48
4.1	GROSS POSTURAL CHANGES	48
4.2	POSTURAL ENGAGEMENT RESULTS.....	53
4.2.1	Changes in Postural Engagement.....	53
4.2.2	Predicting The Level of Postural Engagement.....	60
4.2.3	Principal Component Analysis	62
5.0	DISCUSSION	68
5.1	GROSS POSTURAL CHANGES	68
5.2	POSTURAL ENGAGEMENT RESPONSE	71
5.3	SOURCE OF SEATED POSTURAL CHANGES.....	76
5.4	LIMITATIONS.....	78
6.0	CONCLUSION.....	79
APPENDIX A	TASK SCORING	81
APPENDIX B	CLASSIFIER ACCURACY	85
LITERATURE CITED	95

LIST OF TABLES

Table 1. The order of trials and their waves during the Second Day of Testing	24
Table 2. Conditions that characterize each wave of incoming tracks.....	29
Table 3. Raw Posture Variables.....	30
Table 4. Summary of gross postural changes over all waves (n = 420).	49
Table 5. Differences in n $\bar{N}_6(\tau)$, $\bar{N}_{12}(\tau)$, $\bar{N}_{18}(\tau)$, and $\bar{N}_{24}(\tau)$ throughout a wave.....	59
Table 6. Ability of the mahalanobis classification system to correctly predict $N(\tau)$	61
Table 7. The variance accounted for by the principal components calculated	63
Table 8. Ability of the classifier to reproduce the correct classifications when the observations are defined posture variables in comparison to when they are defined by principal components that account for more that 5.0% of the data’s total variance.	66
Table 9. Points Awarded for Identifying, Querying,	81
Table 10. Maximum possible score for each wave within Trial J.	82
Table 11. Maximum possible score for each wave within Trial K.....	82
Table 12. Maximum possible score for each wave within Trial L.	83
Table 13. Percentage breakdown of predicted $N(\tau)$ values for each subgroup of Known $N(\tau)$ Values ($N(\tau) = [0, 1, 2, 3, 4, 5, \geq 6]$, $X(\tau) = [V(\tau)]$).....	85
Table 14. Percentage breakdown of predicted $N(\tau)$ values for each subgroup of Known $N(\tau)$ Values ($N(\tau) = [0, 1, 2, 3, 4, 5, \geq 6]$, $X(\tau) = [V(\tau), V(\tau-16)]$).....	86
Table 15. Percentage breakdown of predicted $N(\tau)$ values for each subgroup of Known $N(\tau)$ Values ($N(\tau) = [0, 1, 2, 3, 4, 5, \geq 6]$, $X(\tau) = [V(\tau), V(\tau-16), V(\tau-32)]$).....	86

Table 16. Percentage breakdown of predicted $N(\tau)$ values for each subgroup of Known $N(\tau)$ Values ($N(\tau) = [\leq 2, \geq 3]$, $X(\tau) = [V(\tau)]$).....	87
Table 17. Percentage breakdown of predicted $N(\tau)$ values for each subgroup of Known $N(\tau)$ Values ($N(\tau) = [\leq 2, \geq 3]$, $X(\tau) = [V(\tau), V(\tau-16)]$).....	87
Table 18. Percentage breakdown of predicted $N(\tau)$ values for each subgroup of Known $N(\tau)$ Values ($N(\tau) = [\leq 2, \geq 3]$, $X(\tau) = [V(\tau), V(\tau-16), V(\tau-32)]$).....	88
Table 19. Percentage breakdown of predicted $N(\tau)$ values for each subgroup of Known $N(\tau)$ Values ($N(\tau) = [\leq 1, 2-4, \geq 5]$, $X(\tau) = [V(\tau)]$).....	88
Table 20. Percentage breakdown of predicted $N(\tau)$ values for each subgroup of Known $N(\tau)$ Values ($N(\tau) = [\leq 1, 2-4, \geq 5]$, $X(\tau) = [V(\tau), V(\tau-16)]$).....	89
Table 21. Percentage breakdown of predicted $N(\tau)$ values for each subgroup of Known $N(\tau)$ Values ($N(\tau) = [\leq 1, 2-4, \geq 5]$, $X(\tau) = [V(\tau), V(\tau-16), V(\tau-32)]$).....	89
Table 22. Percentage breakdown of predicted $N(\tau)$ values for each subgroup of Known $N(\tau)$ Values ($N(\tau) = [0, 1, 2, 3, 4, 5, \geq 6]$, $X(\tau) =$ Principal Components derived from $[V(\tau)]$ that account for more than 5% of the data's total variance).....	90
Table 23. Percentage breakdown of predicted $N(\tau)$ values for each subgroup of Known $N(\tau)$ Values ($N(\tau) = [0, 1, 2, 3, 4, 5, \geq 6]$, $X(\tau) =$ Principal Components derived from $[V(\tau), V(\tau-16)]$ that account for more than 5% of the data's total variance).....	90
Table 24. Percentage breakdown of predicted $N(\tau)$ values for each subgroup of Known $N(\tau)$ Values ($N(\tau) = [0, 1, 2, 3, 4, 5, \geq 6]$, $X(\tau) =$ Principal Components derived from $[V(\tau), V(\tau-16), V(\tau-32)]$ that account for more than 5% of the data's total variance).....	91
Table 25. Percentage breakdown of predicted $N(\tau)$ values for each subgroup of Known $N(\tau)$ Values ($N(\tau) = [\leq 2, \geq 3]$, $X(\tau) =$ Principal Components derived from $[V(\tau)]$ that account for more than 5% of the data's total variance).....	91
Table 26. Percentage breakdown of predicted $N(\tau)$ values for each subgroup of Known $N(\tau)$ Values ($N(\tau) = [\leq 2, \geq 3]$, $X(\tau) =$ Principal Components derived from $[V(\tau), V(\tau-16)]$ that account for more than 5% of the data's total variance).....	92
Table 27. Percentage breakdown of predicted $N(\tau)$ values for each subgroup of Known $N(\tau)$ Values ($N(\tau) = [\leq 2, \geq 3]$, $X(\tau) =$ Principal Components derived from $[V(\tau), V(\tau-16), V(\tau-32)]$ that account for more than 5% of the data's total variance).....	92
Table 28. Percentage breakdown of predicted $N(\tau)$ values for each subgroup of Known $N(\tau)$ Values ($N(\tau) = [\leq 1, 2-4, \geq 4]$, $X(\tau) =$ Principal Components derived from $[V(\tau)]$ that account for more than 5% of the data's total variance).....	93

Table 29. Percentage breakdown of predicted $N(\tau)$ values for each subgroup of Known $N(\tau)$ Values ($N(\tau) = [\leq 1, 2-4, \geq 4]$, $X(\tau)$ = Principal Components derived from [$V(\tau)$, $V(\tau-16)$] that account for more than 5% of the data's total variance). 93

Table 30. Percentage breakdown of predicted $N(\tau)$ values for each subgroup of Known $N(\tau)$ Values ($N(\tau) = [\leq 1, 2-4, \geq 4]$, $X(\tau)$ = Principal Components derived from [$V(\tau)$, $V(\tau-16)$] that account for more than 5% of the data's total variance). 94

LIST OF FIGURES

Figure 1. Warship Commander Strategic Air space Monitoring Task.	21
Figure 2. Varying task difficulty during four different waves. As the maximum number of tracks on screen during a particular wave increases, it becomes more difficult for the subject to complete the task successfully.	23
Figure 3. Left: Schematic of subject in testing position; Right: Actual prototype postural assessment chair and workstation.	25
Figure 4. Example of a seat pressure profile displayed by an FSA system [25]. The pressure recorded by each of the 256 pressure seat sensors is displayed in a two-dimensional array, and a color-coded interpolation of the pressure distribution is overlaid for display purposes.	26
Figure 5. Left: Seat pressure profile with overlay (green) to highlight the location of the left and right posterior thigh and buttock. The subject is oriented so that $x = 0$ corresponds to the front edge of the seat. Right: Seat pressure profile with overlay highlighting Left Center of Pressure (Left COP), Right Center of Pressure (Right COP), Base of Support (BOS), and Seat Yaw Angle (SY).	32
Figure 6. Example of the moving correlation window. Here, the base of support (BOS) is being correlated with the instantaneous number of tracks on screen in a window centered at data point 160 (35 sec) as is indicated by the dashed red line. The solid red lines indicate the upper and lower temporal boundaries of the window, which spans ± 20 data points.	37
Figure 7. Observation from within the same data set may be segregated into distinct groups.	39
Figure 8. Basic model of a multivariate classifier. The classifier is trained to classify an observation based on the relationship between the training observations (defined by a collection of variables) and their known classifications.	40
Figure 9. Use of classifier in the current study. A mathematical classifier was used to reproduce the known classifications of the training observations.	41

Figure 10. Two-variable principal component example. Variables X_1 and X_2 define 85 observations. A second coordinate system is defined in which the first principal component, U_1 , accounts for the maximum amount of data's variance. The second principal component, U_2 , is orthogonal to U_1 . U_1 accounts for 87.5% of the data's total variance, and U_2 accounts for 12.5% of the data's total variance. 44

Figure 11. Stabilograms depicting how a subject's seated posture varies while completing waves with a maximum of 6 (left) and 24 tracks (right)..... 49

Figure 12. The difficulty of the task significantly affects the total distance traveled by the center of pressure $\log(\Delta COP)$. Standard error bars included. (* significant difference, $p < 0.05$) 50

Figure 13. The difficulty of the task significantly affects the total change in base of support (ΔBOS). Standard error bars included. (* significant difference, $p < 0.05$)..... 51

Figure 14. The difficulty of the task significantly affects the total change in seat yaw (ΔSY). Standard error bars included. (* significant difference, $p < 0.05$)..... 51

Figure 15. Examples of the moving correlation window during a wave of 18 tracks. The left graph illustrates a region of high correlation. Within the window centered at 13.1 sec (data point 60), anterior/posterior seat center of pressure is correlated with tracks on screen with a correlation coefficient of $r = 0.82$. The right graph illustrates a region of low correlation. Within the window centered at 61.3 sec (data point 280), anterior/posterior seat center of pressure is correlated with tracks on screen with a correlation coefficient of $r = 0.20$ 53

Figure 16. Average cumulative postural engagement response, \bar{N} . The average number of posture variables that are highly correlated to tracks on screen is a very dynamic measure of postural engagement. 54

Figure 17. $\bar{N}_6(\tau)$ (top left), $\bar{N}_{12}(\tau)$ (top right), $\bar{N}_{18}(\tau)$ (bottom left), and $\bar{N}_{24}(\tau)$ (bottom right) are plotted with rescaled values of $\bar{t}_6(\tau)$, $\bar{t}_{12}(\tau)$, $\bar{t}_{18}(\tau)$, and $\bar{t}_{24}(\tau)$ respectively. In each case, the maximum value of $\bar{N}_i(\tau)$ occurred during the initial buildup of tracks on screen, followed by a sudden decrease in $\bar{N}_i(\tau)$ prior to tracks on screen reaching its maximum value. Note that $\bar{N}_6(\tau)$ did not increase towards the end of the wave as the other value of $\bar{N}_i(\tau)$ did..... 55

Figure 18. The average number of highly correlated variables varies with task difficulty, with distinct differences occurring up to 25s. 57

Figure 19. Principal components calculated from the observations $X(\tau) = [V(\tau)]$. Plotting the total variance accounted for by each principal component shows there is not a distinct group of principal components that appear to account for random variability. 64

Figure 20. Principal components calculated from the observations $X(\tau) = [V(\tau), V(\tau-16)]$. The first 7 principal components each account for more than 5.0% of the total variance and collectively account for 89.3% of the total variance..... 65

Figure 21. Principal components calculated from the observations $X(\tau) = [V(\tau), V(\tau-16), V(\tau-32)]$. The first 5 principal components each account for more than 5.0% of the total variance and collectively account for 76.4% of the total variance..... 65

Figure 22. Segmenting the cumulative postural engagement response (\bar{N}). By examining \bar{N} calculated for waves with *wave type*₆, *wave type*₁₂, *wave type*₁₈, and *wave type*₂₄, waves can be segmented into an initial phase (0 to 25 sec), middle phase (25 to 50 sec), and end phase (50 to 75 sec)..... 72

Figure 23. The average percentage of the maximum possible number of points awarded during different *wave types*. Standard error bars included..... 83

Figure 24. The average percentage of the maximum possible number of points awarded during different *trial types*. Standard error bars included. 84

NOMENCLATURE

$BOS(\tau)$	Base of Support: the distance between centers of pressure formed by the left and right ischial tuberosities at data point τ
ΔBOS	Change in Base of Support: the absolute change in base of support (BOS) between sequential time points summed throughout the testing period
C	Column: one column of the seat pad or back-pad pressure matrix
$COP(\tau)$	Center of Pressure: the center of pressure of the seat pad/buttock interface or the back-pad/back interface at data point τ
ΔCOP	Change in Center of Pressure: the absolute change in position of the seat center of pressure (COP) between sequential time points summed throughout the testing period
$COP_{Left}(\tau)$	Left Center of Pressure: the center of pressure of the left half of the seat-pad/buttock interface at data point τ
$COP_{Right}(\tau)$	Right Center of Pressure: the center of pressure of the right half of the seat-pad/buttock interface at data point τ
D	The mahalanobis distance between groups of observations in multidimensional scaling
$M(\tau)$	A matrix representing the 16x16 array of pressure data recorded by pressure sensors in the seat pad or back-pad at data point τ
$N(\tau)$	The number of posture variables that are highly correlated to the number of tracks on the screen within a defined window of time centered at data point τ
ρ	The rotation matrix used to transpose posture variables to principal components
R	Row: one row of the seat pad or back-pad pressure matrix
$r_i(\tau)$	The correlation between the posture variable i and the instantaneous tracks on screen within a defined window of time centered at data point τ

$SY(\tau)$	Seat Yaw: the angle formed by the vector connecting the centers of pressure formed by the left and right ischial tuberosities and the front edge of the seat at data point τ
ΔSY	Change in Seat Yaw: the absolute change in seat yaw (SY) between sequential time points summed throughout the testing period
$SSY(\tau)$	Sine of Seat Yaw: the sine of the seat yaw (SY) at data point τ
T	The total number of data points in one wave of a trial (343 data points)
τ	An individual data point within a wave
$t(\tau)$	The number of tracks on screen in the Warship Commander Task at data point τ
U	The collection of principal components derived from the seated posture variables
U_i	One specific principal component derived from the seated posture variables
$V(\tau)$	The original set of posture variables (Table 3, pp 30)
X	The collection of observations defined at all data points based on seated postural measures
$X(\tau)$	An observation at data point τ that is defined by the variables χ_1 through χ_n
X_g	A group of observations making up X that have been assigned to a particular group g based on common values of $N(\tau)$
χ_n	A variable used in defining the observations X that represents one of the posture variables $V(\tau)$, or its history
x	Anterior/posterior position in reference to the seat pad center of pressure and the back-pad center of pressure
y	Medial/lateral position in reference to the seat pad center of pressure and superior/inferior position in reference to the back-pad center of pressure

1.0 SPECIFIC AIMS

The long term goal of this project is to devise a completely unobtrusive means of gauging changes in a seated computer operator's cognitive state that are due to changing task conditions. Constructing such a gauge will make it possible to detect scenarios in which (a) there is a risk of exceeding the operator's cognitive abilities and (b) the operator is not properly aware of the task conditions. Avoiding such scenarios reduces the likelihood of catastrophic task performance. Specifically, this thesis proposes that dynamic seated posturography can identify specific postural responses that are indicative of an operator's level of engagement in a task and awareness of the task conditions.

It has been demonstrated in several past studies that increasing the difficulty of a cognitive task correlates with quantifiable standing postural changes. However, most real-life tasks that require an operator to make decisions based on rapidly-presented information are performed by seated operators, such as air-traffic controllers and motorists. Although changes in seated posture due to increased cognitive demands have been investigated, current research is based largely on non-quantified evaluation of posture such as nonverbal communication. Therefore, it is the objective of this thesis to **1)** quantitatively measure seated posture during task performance and identify specific alterations that can be correlated to task difficulty and **2)** use the aggregate of these postural alterations to construct a mathematical classifier that is capable of predicting the contexts of the task.

Specific Aim 1: To provide measures based on the distribution of pressure over the seat which demonstrate that seated posture is altered in response to the increased cognitive demands of a simulated air-space monitoring task.

H.1 While performing a simulated air-threat monitoring task, changes in a subject's seated posture that occur over the course of an entire trial can be correlated to the trial's level of difficulty. Such measures are based on the change in position of the seat-buttock interface center of pressure and the position of the left and right buttocks center of pressure with respect to each other, representing a seated base of support.

Specific Aim 2: To predict the contexts of a simulated air-space monitoring task in real-time by classifying changes in a collection of seated posture variables.

H.2 The alterations in seated posture exhibited by subjects throughout the course of a trial can be used to predict the changing contexts, and subsequent changing difficulty, of the simulated air-threat monitoring task.

2.0 BACKGROUND AND SIGNIFICANCE

2.1 SCOPE OF THE PROBLEM

The emphasis placed on military and civilian workstation operators (e.g. computer users, motorists) to multitask has increased with the advancement of computer technology. For example, a motorist may simultaneously process information regarding traffic patterns, incoming phone calls, and a navigation system. Military personnel may be asked to operate multiple unmanned aircraft at one time. What must be considered by those who design the workstation interfaces is that the amount of information one is capable of processing at any moment is limited [26, 58]. Human information processing capabilities have therefore become the constraining factor in human/machine interaction [52]. Although placing excessive cognitive demands on an operator is detrimental to proper task performance, current human/workstation interfaces are not sensitive to the operator's cognitive limitations except through performance statistics. It would therefore be advantageous to develop a system capable of probing the operator's cognitive state and subsequently modifying task presentation and objectives so as to maximize productivity [58]. This would potentially allow the system to detect that the operator is close to exhausting his or her cognitive capabilities or is not prepared to perform the task before performance degrades.

Military and industrial sources predict that, in the coming decades, significant research and development efforts will be devoted to improve user/workstation interfaces to make them

more aware of the user's cognitive needs and abilities [16]. To date, progress in developing closed loop user/machine systems has largely been made due to The Defense Advanced Research Projects Agency's (DARPA) Augmented Cognition program (AugCog). The objective of the AugCog program is to extend "the information management capacity of the human-computer warfighting integral by developing and demonstrating quantifiable enhancements to human performance in diverse, stressful, operational environments" [8].

As members of the AugCog program, our research group investigates means of implicitly gauging cognitive state, while other members investigate using this information to enhance task performance. In order to best serve the objectives of the AugCog program, such cognitive state gauges must (a) be capable of operating in nearly any environment, (b) be compatible with other sensors, (c) provide meaningful data in real-time without the need for post-collection analysis, and (d) be effective regardless of the subject population [32, 52, 57]. In addition, the means of gauging cognitive state should not interfere with an operator's ability to perform the given task in a natural manner due to setup/calibration requirements or any means of physically interfering with them, as it would impede productivity.

2.2 RESEARCH BACKGROUND

2.2.1 Cognition and Task Performance

The present study aims to identify seated postural changes that are associated with changes in cognitive state that occur while an operator updates his or her awareness of a given task. This awareness of surrounding conditions that a person develops to complete a task is referred to in human factors literature as situational awareness. Endsley [21] states that developing this

understanding is dependent on: (1) perception of information; (2) comprehension of the information within the contexts of the situation. Endsley further suggests that developing situational awareness is a precursor to all decision making and subsequent action during task performance. Therefore, it is necessary to maintain a certain level of awareness of task conditions in order to properly complete the task, which can be cognitively demanding.

The definition of situational awareness is very broad, and it can encompass a wide range of cognitive activity. However, our ability to develop an understanding of a given situation is intuitively dependent on perception of information. It is therefore reasonable to conclude that the structure of situational awareness is dependent on how humans perceive events. Zacks et al [64] researched the structure of event perception by studying subjects while they viewed videos of actors performing common goal-oriented tasks (e.g. making a bed). During the first viewing of the video, fMRI images of the brain were acquired while subjects passively viewed the video. During two successive viewings, subjects identified (a) the beginning and end of what they perceived as the smallest meaningful units of the task during one viewing, and (b) the beginning and end of what they perceived as the largest meaningful units of the task during the other viewing. Based on differences in cortical activation responses, it was concluded that perception of the small units is in fact distinct from perception of large units. Furthermore, in a separate study performed by Zacks et al [65], it was concluded based on the temporal alignment of unit boundaries that these units are hierarchically structured: The perception of large units of a task can be broken down into the perception of the small units.

Just as event perception has been defined by the hierarchical structure of large and small event units, situational awareness can be divided into analogous components, termed global and local awareness [10, 31]. Global awareness represents an operator's perception, understanding,

and prediction of the task as a whole, and it is influenced by the collective interactions of all subtasks making up the task. Local awareness represents an operator's perception, understanding, and prediction of each of the subtasks. Consider the task in the present study in which operators are required to monitor a simulated air space. An operator must identify all incoming tracks (aircraft) and decide whether to ignore them or neutralize them based on their identified threat level and bearing. At a given moment, an operator will have developed a local awareness based on identifying and assessing a specific track. In addition, the operator would also have developed a global awareness of the general condition created by all of the tracks on screen (i.e. busy, calm, under attack).

Tasks with rapidly changing contexts require operators to make decisions frequently. Doing so requires constant update of global and local awareness of the situation. In such tasks, maintaining proper situational awareness can require a major effort from the operator, which is especially true when the operator lacks substantial task experience [21]. Therefore, updating situational awareness is more cognitively demanding during a highly dynamic task than a less dynamic task.

2.2.2 Current Gauges of Cognition

The current study proposes that measuring dynamic seated posture will help to gauge changes in cognitive state pertaining to task completion. Other means of gauging changes in cognitive state have already been developed, although there does not yet appear to be a standard for doing so. In addition, the current means of gauging cognitive state are not yet suitable for use in real-world workstations.

Assessment of cognitive state is dependent on the use of psychophysiological sensors that provide explicit and implicit measures of neural activity [57]. Explicit measures have the potential to reflect activity in specific regions of the brain, which would allow us to infer cognitive state based on our knowledge of functional neuroanatomy. Implicit cognitive state cues measure motor consequences of brain activity.

Explicit measures of neural activity record brain activity via continuous and event related electrical encephalography (EEG), Positron Emission Tomography, functional Magnetic Resonance Imaging, and functional Near Infrared Spectroscopy [12, 20, 57, 58]. It has been demonstrated that EEG can be used to successfully derive measures indicative of workload and perceived difficulty [12, 20]. Since EEG analyses have classically been associated with complex sensor configurations that require significant processing and hinder task performance due to physical constraints, much work has been performed to develop simplified EEG systems that can be practically used in real-world workstations.

Duta et al [20], for example, developed a neural network model that is capable of successfully gauging vigilance, an important factor in probing cognition, using only mastoid channel EEG. This offers a great advantage over other systems that require EEG, EMG, and EOG input for vigilance monitoring. Berka et al [12] were similarly able to detect changes in neural activity involved in alertness and cognitive workload using a new lightweight, wireless EEG system with fixed-position sensors. While such findings are very promising in our attempt to infer cognitive state, EEG analysis is not yet capable of serving as a lone cognitive state gauge that can be used to enhance task performance. EEG data is highly susceptible to being plagued with artifact caused by muscle activity or sensor movement. In Duta et al's study, only 80% of the mastoid channel data collected to train the model was reported as artifact free.

Other investigators have therefore turned their attention to developing indirect means of inferring cognitive state that may compliment or possibly even replace systems that rely on explicit measures of neural activity. Such measures include eye movement, pupil dilation, heart rate, and galvanic skin response [32, 57]. Hoover et al [32] developed a cardiovascular index of the autonomic nervous system, in which changes in respiratory sinus arrhythmia are measured in order to quantify vagal activity. In comparing tasks with various difficulty levels to rest state, they were able to demonstrate a significant difference in arousal level between rest state and the most difficult level of task. However, it is likely a more sensitive and selective measure of arousal measurement will be required to effectively augment an operator's task performance.

Current measures of cognitive state lack precision, and in addition the sensors used to probe cognitive state can not yet be feasibly used in real-world operational environments. Current sensors often have physical limitations (e.g. size, tethering), and require extremely precise placement for accurate data collection and significant calibration time.

A robust psychophysiological cognitive state cue that can be monitored in a completely unobtrusive manner has yet to be identified. Past research has reported that performance of cognitive tasks is accompanied by various specific changes in human posture. Given the current state of motion tracking technology, such postural changes that occur during cognitive task performance can be monitored in a completely unobtrusive manner. Therefore, researchers have begun to investigate whether dynamic posture can serve as an effective cognitive state cue that can be used for augmenting cognitive task performance.

2.2.3 Cognition and Standing Posture

Most research that focuses on the relationship between cognition and postural control concentrates on standing postural control. Although the present study is concerned with changes in seated posture, studying standing posture literature provides examples of how cognition-dependent postural changes have been quantified.

Current models that define the integration of neural input required to maintain stable standing posture include some level of cognition [33, 34, 46, 47]. Although there is no specific neuro-anatomical basis for hypothesizing that cognition is imperative for maintaining posture or that substantial cognitive processing can interfere with postural control, EEG has been used to demonstrate how cortical activity changes when a postural task and cognitive task are performed concurrently. Quant et al [46] reported changes in the N1 response (a distinct cortical activation pattern measured using scalp EEG electrodes that is observed 100 to 200 ms after exposure to a postural perturbation) when standing subjects performed a visual tracking task while being subjected to horizontal perturbations. Combining the postural task and the visual tracking task resulted in a decrease in the magnitude of the N1 response (though no temporal delay was evident) and a subsequent increase in center of pressure (COP) excursion when compared to performing the postural task alone. The increase in COP excursion demonstrates that subjects' postural control strategies are altered in response to performing dual cognitive/postural task. It was concluded that the diminished N1 response is the result of a reduction in available cognitive resources, and therefore posture-related cortical activity is altered in response to increased cognitive demands.

Rather than seeking anatomic evidence to better understand the role of cognitive engagement in postural tasks, most postural control literature studies alterations in performance

that are exhibited when cognitive tasks and postural tasks are performed concurrently. The two main hypotheses driving such testing are: (a) postural tasks and cognitive tasks compete for common supraspinal resources which are limited [7, 14, 28, 36, 62]; (b) attentional shifts occur as subjects redefine which of the two tasks is primary and which is secondary [38, 43, 48]. Regardless of which (or if either) hypothesis is correct, it is commonly found that performance will be altered in the postural task, the cognitive task, or both when the combined effort requires a sufficient amount of attention.

Typically, the stability of standing posture is quantified using a force-sensing platform to measure changes in position of the ground-foot interface center of pressure (COP) [45]. Although healthy humans are typically capable of maintaining steady-state balance, quiet standing is still characterized by small changes in COP due to movement about the ankle and hip [61]. This movement is typically referred to as postural sway. The comparison of postural sway in healthy subjects and patients during both quiet and perturbed stance is used as a means of objectively evaluating postural deficits. For instance, monitoring abnormalities in postural sway patterns has been used to study diminished postural control in Parkinson's patients [13, 39], vestibular deficient patients [3], and elderly subjects [4, 54].

Studying changes in sway patterns with respect to simultaneously presented postural tasks and cognitive tasks, referred to as a dual task paradigm, has proven useful in attempting to more clearly define the role of cognition in postural control. Dual task paradigm studies recognize altered posture and task performance as dependent variables and the difficulty and modality of the postural and cognitive tasks as independent variables [63]. The difficulty of the postural task may be altered by introducing perturbations [14, 43, 48], sway referencing [7], muscle stimulation [5, 6], unstable stance position [7, 36, 40], or having subjects perform a gait

task [36]. Testing patients with impaired balance also increases the variability of postural control [6, 7, 14, 27, 28, 39]. Researchers have also used a variety of cognitive task modalities, including mathematical [5, 6, 27, 28, 37, 39], auditory and visual reaction time [14, 36, 48], visual association [27, 40], and visual tracking tasks [38, 43]. Subjects with impaired cognitive abilities, such as Alzheimer's patients, have been used in order to introduce variability [50].

Dual task studies often focus on increasing the difficulty of the postural task and observing subsequent changes in performance of both the postural and cognitive tasks. Andersson et al [7] had healthy subjects and balance-impaired patients perform a visuospatial memory task in a seated position and while standing on a sway-referenced platform (designed to reduce proprioceptive information from the ankle) with eyes open and with eyes closed. It was found that healthy subjects were significantly less likely to perform the task correctly while standing with eyes opened or closed compared to the seated condition, and patients were significantly less likely to perform the task correctly while standing with eyes closed when compared to the seated condition. While cognitive performance results were similar between groups when the postural task became more difficult, postural performance differed: Sway increased in control group subjects when the memory task was introduced but sway decreased in patients.

In a separate study by Andersson et al [6], healthy subjects and balance impaired subjects were asked to count backwards by seven for twenty seconds while being subjected to vibratory calf stimulation. Similar to Andersson's previously cited study [7], it was found that patients exhibited less anterior-posterior sway while performing the dual task compared to the postural task alone.

Brauer et al [14] presented healthy and balance-impaired older adults with an auditory reaction time task with simultaneous translational perturbation. In the dual task scenario, balance-impaired adults completed the cognitive task with increased reaction time compared to healthy subjects. Unlike Andersson et al's studies [6, 7], impaired patients took longer to stabilize their balance following perturbation in the dual task scenario compared to perturbation alone, which implies that postural control had suffered in response to the cognitive task.

The deterioration of cognitive task performance that accompanies increased postural demands observed in these studies helps us to conclude that maintaining balance does tax cortical resources. However, postural performance results are often inconsistent across such studies [49]. Maki et al [37] propose that dual tasks invoking heightened arousal versus heightened attention may yield different postural results. Maki et al define attention as, "a focusing of cognitive resources on a specific task," (p. 54) and arousal as, "a non specific state of readiness to respond" (p. 54). Perturbation tasks require subjects to prepare to react very quickly to an unexpected change in postural demands, which heightens arousal according to Maki et al's definition. Standing on a sway-referenced platform, on the other hand, requires increased attention due to continuous readjustment throughout the entire trial. Although attention and arousal are states that are difficult to define, this might help to explain differences in results reported in such studies.

Unlike the previous three studies, the experiments performed by Maki et al [37] only used the cognitive task as an independent variable without applying any type of postural perturbations. Standing in a wide-based stance to insure postural stability, healthy young adults were presented with various listening tasks intended to elicit attention, arousal, or both. Skin conductance was measured in an attempt to quantify arousal, and subjects were asked to evaluate

their anxiety as a subjective measure of arousal. While performing a math task, which was intended to raise arousal and attention, it was found that subjects who reported experiencing a high level of anxiety demonstrated a direct correlation between skin conductance and an anterior shift in COP.

In a similar study, Melzer et al [40] performed dual task testing in which healthy young and older subjects were asked to perform a visual association task (a modified version of the Stroop test). The only variability in the postural task was that subjects stood with both wide (easy) and narrow (difficult) bases of support. It was reported that young subjects standing with a narrow base of support had an increased COP path length and mean COP velocity, implying decreased postural stability, while performing the cognitive task compared to quiet stance alone. Older subjects standing with a narrow base of support, however, demonstrated a decrease in COP area, implying improved postural stability, while performing cognitive task compared to quiet stance alone. What is more interesting is that with both groups standing in a stable, wide-based position, COP path length, elliptical area, and sway velocity all increased when comparing dual task to single task. Although it is again difficult to identify postural tendencies in these studies due to variability of cognitive tasks and subject populations, it has been demonstrated that increasing cognitive demands results in altered posture even when the postural task is as simple as wide-based standing! This further proves how sensitive postural control strategies are to increased cognitive demands.

Due to the lack of clinical significance, very little research has been devoted to studying supraspinal contributions to seated postural control. Standing posture is less stable than seated posture due to increased physical demands and the integration of more sensory information. Patients with vestibular impairments are severely more hindered, and subsequently are at higher

risk of suffering injury while attempting to maintain standing balance than seated balance. Similarly, older adults often have a history of repeated falls that occur during gait due to impaired upright maintenance of balance. In the standing postural control literature, seated posture is even considered stable enough to use as a control condition [7, 36]. However, the relationship between seated posture and cognition has long been studied in nonverbal communication research [15, 19, 30, 53]. Recent interest in gauging the cognitive state of seated operators has also led researchers to investigate the use of cognition-dependent seated postural changes to develop such a gauge [10, 41, 42].

2.2.4 Cognition and Seated Posture

2.2.4.1 Nonverbal Communication

As humans, we commonly monitor the motions of others people in order to evaluate task performance [51] and to provide structure to our perception of task performance [56]. In a study performed by Speer et al [56], subjects passively viewed films of actors performing common goal oriented tasks while cortical blood flow was measured using magnetic resonance imaging (MRI). Subjects then viewed the videos again and were instructed to identify when they felt meaningful segment boundaries occurred. By examining the MRI images at instances at which subjects reported segment boundaries, it was found that reported segment boundaries were temporally aligned with spikes in cortical activity in the extrastriate-motion complex, a region of the cortex associated with motion perception. They concluded that humans monitor motion cues to structure event perception. Since we depend on changes in human motion to help assess task performance, it is logical that we in turn use postural changes to convey information. For this

reason, humans often change their posture as a means of nonverbally conveying information [15].

Nonverbal communication is often associated with facial expressions and hand gestures; however, humans also communicate through easily-recognized postural changes [15, 17, 19, 30, 53]. Shapiro [53] states that while facial expressions are used to express specific emotions, posture can be used to express the range of emotion intensity. In addition, postural changes can be used to provide information regarding the structure of task performance, as has been demonstrated in studies of human dialogue [15, 17]. Bull [15] states that such forms of nonverbal communication may occur without conscious intention and without awareness of how significant the cue may be. Therefore, posture can provide information to an observer that is not conveyed through speech or task performance.

Cassell [17] and Bull [15] have reported that changes in posture are used during dialogue to help structure conversation and convey intentions. Based on observations made of subjects engaged in dialogue, Cassell [17] reported that postural shifts (defined as body motion excluding hand and eye motion) occur more frequently as the speaker nears the end of what he or she is saying. In addition these postural shifts are significantly longer when the speaker is ending the discussion compared to when the speaker is turning discussion over to someone else. Bull [15] similarly reported that seated posture serves as a cue to indicate turn-taking during dialogue. He additionally reported that pre-speech posture provides information regarding the nature of the speech. For example, subjects were more likely to turn their head away from the other speaker prior to replying to them and were more likely to raise their head up prior to making a request.

Posture can also be used to infer the level of interest of someone performing a task. Bull [15] monitored alterations in seated posture while subjects viewed video excerpts which they

classified as being interesting or boring. It was reported that subjects were significantly more likely to lean forward during excerpts that they found to be interesting than during excerpts that they found to be boring. Conversely, subjects were significantly more likely to lean backwards during excerpts that they found to be boring than during excerpts that they found to be interesting. In addition, subjects were significantly more likely to change head orientation during boring excerpts than interesting excerpts.

Although studies of posture as nonverbal communication clearly demonstrate that we use easily-observed seated postural changes to consciously and subconsciously provide those around us with information regarding our cognitive state, they rarely quantify seated postural changes. Due to the current state of motion assessment technology, recent studies have presented means of automating recognition of specific seated posture profiles based on the distribution of seat and back pressure [41, 42, 60]. This in turn has enabled Mota et al [41, 42] to automate the process of inferring cognitive state based on seated postural changes, which is the objective of the current study.

In the study performed by Mota et al [42], the interest levels of children playing a video game were identified by teachers based on their assessment of the children's nonverbal communication. Possible interest levels included: high interest; low interest; and taking a break. Pressure-sensitive seat pads were used to measure the distribution of pressure over the seat. A feed-forward neural network was trained to classify the resulting pressure profiles throughout the trial as: sitting on the edge; leaning forward; leaning forward to the right; leaning forward to the left; sitting upright; leaning backwards; leaning back right; leaning back left; slumping back. A set of Hidden Markov Models was trained to predict the identified interest levels based solely on dynamic sequences of postures. These models were able to predict the interest levels of children

(as identified by the teachers) with 76.5% accuracy when testing children who were not used in training the models.

Mota et al [42] present a novel and effective means of inferring cognitive state; however, the accuracy with which interest level can be predicted is limited by the ability of observers to accurately assess nonverbal communication and the effectiveness with which subjects nonverbally communicated. An alternative that may circumvent these limitations is to evaluate postural changes with respect to the contexts of the task (i.e. task difficulty or urgency), as has been done in the standing posture literature. It is important, however, to note that this approach makes the assumption that a subject's cognitive state is always correlated to the contexts of the task.

Mota et al's [42] cognitive state gauge is also limited in that seated posture is analyzed solely on nine classifications of seated posture. It therefore does not detect small-scale changes in seated posture that may occur due to changing cognitive demands. Pfungst [44] reports that small-scale involuntary changes in posture, such as head and eye movement, are commonly used by humans to convey information even though they are nearly impossible to recognize as non-verbal communication by other human observers. The standing posture literature cited above further supports that cognition-dependent changes in posture may occur on a very small scale. As noted, alterations in standing posture are typically reported as changes in the position of the ground-foot interface COP; however, it is difficult to interpret the absolute scale of full body postural changes based on this measure alone. Hauer et al [28] better demonstrated the small-scale nature of these postural changes by comparing the mean range of the postural sway angle (presumably about the ankle) exhibited by cognitively impaired patients during quiet stance and while performing a mental arithmetic task. Performing the cognitive task was reported to have a

profound effect on the postural control, which was characterized by a 0.6° increase in mean medial/lateral sway and 0.35° increase in anterior/posterior sway.

2.2.4.2 Small-Scale Changes in Seated Posture

Very little literature exists that attempts to quantitatively investigate changes in seated posture. In order to exploit the full potential of seated posture as a cognitive state gauge, the current study proposes to track changes in seated posture with a higher level of spatial resolution so as to monitor large-scale changes in addition to small-scale changes.

It appears that a study performed in part by our research group is the only source that investigates whether seated operators exhibit small-scale postural changes as cognitive demands increase. In the study performed by Balaban et al [10], head translation in the anterior/posterior direction was tracked while operators performed the same simulated air space monitoring task used in the present study (introduced in section 2.2.1). It was reported that while the number of tracks on screen increased during the first half of the trial, operators moved their heads 1-10 mm closer to the computer monitor on which the task was presented. Based on this change in head movement, it was concluded that during this initial phase of the trial head position is linearly related to task difficulty, which is dictated by the total number of tracks on screen.

As previously mentioned, the primary means of identifying small-scale changes in standing posture is by tracking the ground/foot interface COP. Many authors investigating dynamic seated posture have been able to accurately track the COP of the seat/buttock interface using either force plates or pressure-sensitive pads [11, 18, 22, 23, 29, 55]. However, COP tracking has not yet been used in studying the effect of increased cognitive demands on seated posture changes.

3.0 METHODS

3.1 SUBJECT POPULATION

Fifteen subjects performed a computer simulated air space monitoring task while seated in a posture assessment chair. The subject population was limited to healthy adults between the ages of 18 and 45. The health of the subjects was characterized based on self-reported history of neurological or vestibular disorders, and any physical or mental impairments that would preclude computer use and prolonged sitting. These criteria were in place to recruit subjects that are representative of the naval personnel population.

The results reported in this study are based data collected from 14 subjects. An additional subject was tested, but their data was not analyzed due to equipment malfunction and data synchronization errors. The remaining fourteen subjects ranged in age from 20 to 34 years, with a mean age of 23 ± 4 years. Of these subjects, seven were female (mean age: 23 ± 2 years), and seven were male (mean age 24 ± 5 years). All subjects were asked to carefully read and sign a University of Pittsburgh Institutional Review Board-approved informed consent form. The purpose of this was to inform them of the goals of the study, all risks and benefits associated with the experiment, and their rights as participants. After having any questions regarding the study answered by the approved University of Pittsburgh students conducting the experiment, subjects consented to performing the experiment.

3.2 EXPERIMENTAL DESIGN

3.2.1 Cognitive Task

3.2.1.1 Warship Commander Protocol

The cognitive task used in this study was a strategic air space monitoring computer simulation task developed by DARPA titled Warship Commander Task (WCT) (Figure 1). St. John et al [57] used this air space monitoring task in a previous dual task study that integrated 20 different psychophysiological measures of cognitive state. Based on their analysis of subjects' performance statistics and early-stage analyses of the psychophysiological measures, it was found that varying the different WCT difficulty variables significantly affected one's ability to perform the task successfully.

In this task, subjects were presented with twelve consecutive 75.0 sec testing segments, during which a wave of tracks (aircraft) approached the ship's defensive perimeter, or line of engagement. The subject's objective was to identify all incoming tracks, warn any tracks considered to be hostile if they entered the defensive perimeter surrounding the home ship, and neutralize them if they did not leave the defensive perimeter within 3.0 sec.

Once each 75.0 sec wave commenced, the subject was instructed to first identify the threat level each incoming track as (a) friendly, (b) hostile, or (c) unidentified. This was accomplished by tracking an aircraft using the computer mouse, and then highlighting the track using the left mouse button. After a track was highlighted, its threat level could be identified by using the left mouse button (left-click) to select the "Identify Friend or Foe" (IFF) interrogation command on the operator's tool bar. Once the threat level of the track was reported, the track's color would change from gray to blue if it was friendly, red if it was hostile, or yellow if its

threat level was unidentifiable. In addition, its respective threat status would appear on the communication screen when the aircraft's track number was selected on the tool bar.

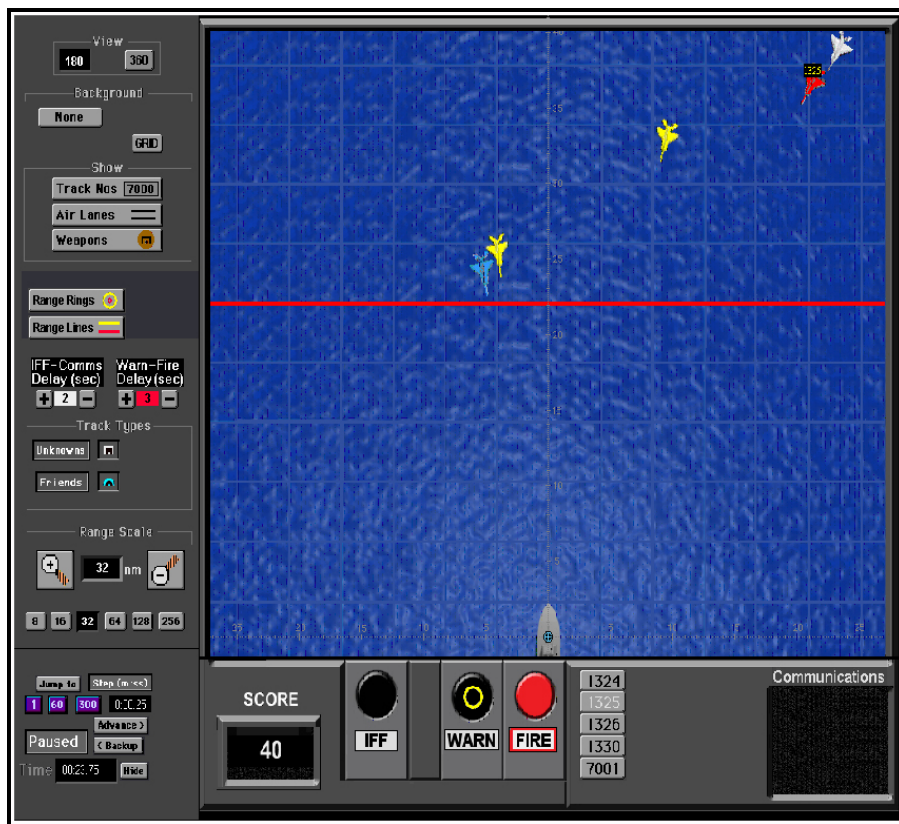


Figure 1. Warship Commander Strategic Air space Monitoring Task.

If a track was identified as being hostile and within the home ship's defensive perimeter, it is to be warned to leave the area by left-clicking the track and using the "Warn" command on the operator's tool bar. The subject was then instructed to permit the hostile track 3.0 sec to leave the defensive perimeter before neutralizing it using the "Fire" command on the operator's tool bar. Any track identified as being friendly was not to be warned or fired upon. The assumed threat level of unidentified tracks was presented to the subject on the

“Communications” screen once the subject left-clicked on the aircraft’s track number on the tool bar at least two seconds after it was identified via the IFF command. Once the assumed threat level of the unidentified track was reported to the subject as either friendly or hostile, it was to be dealt with using the appropriate protocol for the threat level.

The difficulty of WCT was varied throughout the trial in order to vary cognitive workload. This was achieved by modifying (a) the number of tracks in a wave (6, 12, 18, or 24), (b) the ratio of unidentified tracks to friendly/hostile tracks, and (c) secondary auditory information intended to tax verbal memory, which the subjects were instructed to ignore for this particular study (Figure 2). The previous study performed by St. John et al [57] shows that each one of these three effects significantly affects task performance.

In order to correlate psychophysiological measures to task difficulty, the WCT software logged second-by-second contextual information regarding stimuli presentation and performance statistics. Stimuli information included measures such as the instantaneous number of tracks on the screen, the number of tasks pending, and an index of urgency that is based on the weighted sum of pending tasks and their bearings. One recorded performance statistic was the score achieved by the operator within a certain wave. This score was based on the number of tracks in the wave that were identified, warned, and neutralized correctly according the above protocol. Appendix A explains how task performance was scored in more detail.



Figure 2. Varying task difficulty during four different waves. As the maximum number of tracks on screen during a particular wave increases, it becomes more difficult for the subject to complete the task successfully.

3.2.1.2 Trial Sequence

Subjects completed two testing sessions over the course of two days. The first day served as an approximately one hour training session. During this time, the purpose of the study and all risks involved were explained to subjects. Subjects also completed practice rounds of the WCT task while no data was collected.

The second day served as the data collection session, during which time subjects completed four testing trials: practice, J, K, and L. Only results from data recorded during trials J, K, and L are reported in this study. Each of these trials were comprised of twelve consecutive

75.0 sec waves of incoming tracks: three occurrences of waves with a maximum of six tracks to track, three occurrences of waves with a maximum of 12 tracks to track, three occurrences of waves with a maximum of 18 tracks to track, and three occurrences of waves with a maximum of 24 tracks to track (Table 1). The trials varied in that trial K consisted of 67% unidentified tracks and trials J and L consisted of 33% unidentified tracks. Because unidentified tracks require more complex processing due to their ambiguity, it is more difficult for subjects to complete trial K successfully than trials J and L. Subjects were permitted to leave the chair and testing room between rounds as desired, and they were encouraged to do so between rounds J and K.

Table 1. The order of trials and their waves during the Second Day of Testing.

Trial	Maximum Number of Tracks on Screen During a Wave											
Practice	6	6	6	12	6	12	NA	NA	NA	NA	NA	NA
1. J	6	18	12	24	6	18	12	24	6	18	12	24
BREAK												
2. K	6	18	12	24	6	18	12	24	6	18	12	24
3. L	6	18	12	24	6	18	12	24	6	18	12	24

3.2.2 Experimental Equipment and Environment

3.2.2.1 Postural Assessment Hardware

All dynamic posture data was collected using a prototype Dynamic Postural Assessment Chair (Figure 3). This prototype is an operator's chair from Lockheed–Martin's Sea Shadow ship that has been outfitted with seat pad and back-pad slip covers containing ultra thin 16 in × 16 in pressure sensing arrays (VERG, Vista Medical Ltd., force sensitive applications pressure mapping pads). Both the seat and back pressure sensing arrays contain 256 resistive pressure sensors that are capable of collecting up to 200.0 mmHg with a resolution of 0.1 mmHg (Figure 4).

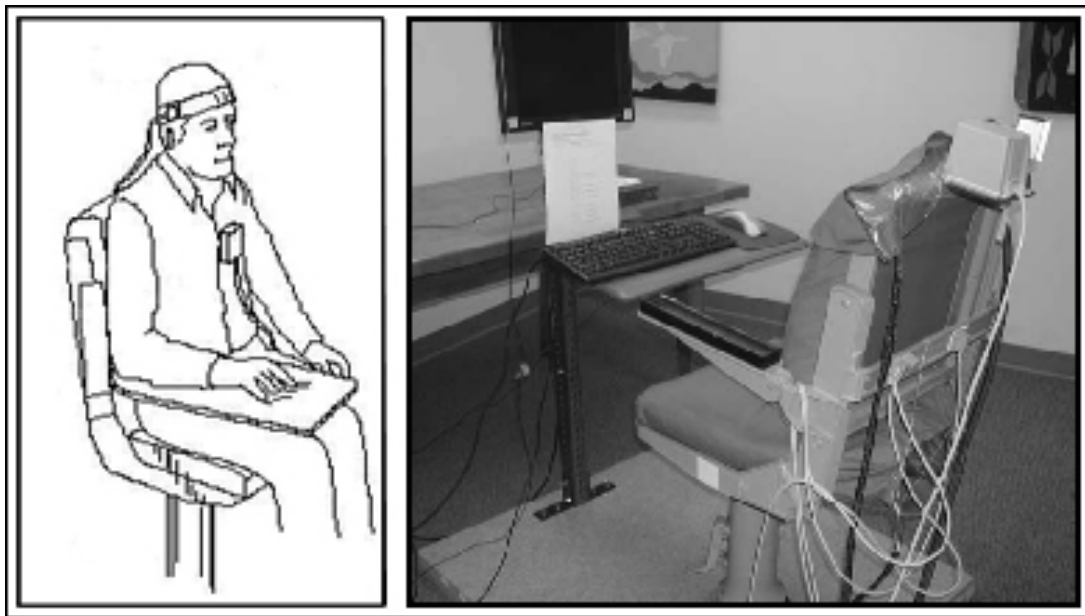


Figure 3. Left: Schematic of subject in testing position; Right: Actual prototype postural assessment chair and workstation.

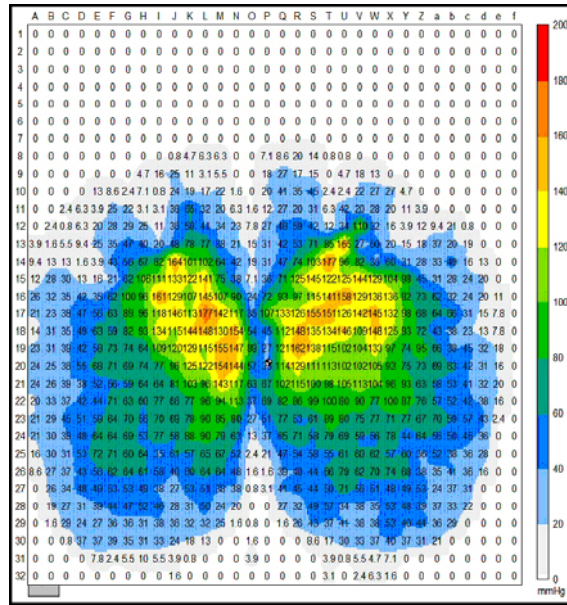


Figure 4. Example of a seat pressure profile displayed by an FSA system [25]. The pressure recorded by each of the 256 pressure seat sensors is displayed in a two-dimensional array, and a color-coded interpolation of the pressure distribution is overlaid for display purposes.

Data was collected at a rate of 4.57 Hz. The distribution of seat pressure was qualitatively analyzed prior to data collection to ensure that the sensors were not overly saturated (i.e. minimal sensors reading 200.0 mmHg) due to subjects having objects (e.g. wallet) in their pockets that could potentially cause miscalculation of posture variables. Similar systems produced by Vista Medical Ltd. have been proven to be reliable and capable of accurately measuring the location of the ischial tuberosities [2].

Using these seat pads allowed us to calculate various seated posture measures that are dependent of the distribution of seat pressure, such as seated COP. Typically, rigid force plates are used to track standing COP, and so others investigators have constructed chairs using force plates as seat pads in order to track seated COP [11, 18, 55]. Although these systems avoid problems encountered when using pressure-sensitive seat pads, such as pad creasing and shifting,

they are not appropriate for the current study. Unlike force plates, the pressure-sensitive seat pads used in the current study have a very low profile and are capable of conforming to the shape of any seat. This makes them completely unobtrusive and exceptionally easy to integrate into real-world workstations. In addition, the dense array of pressure-sensors that is embedded in the pressure-sensitive seat pads allows the distribution of pressure to be monitored various regions of the seat surface. This enables us to calculate the centers of pressure created by the left and right ischial tuberosities, which is necessary for calculating the seated base of support and torsion of the pelvis in the transverse plane.

A magnetic motion tracking system (Flock of Birds, Ascension Technology Corp.) was used to monitor the position and orientation of the head and trunk (mid-sternum) with 6 degrees of freedom at 103 Hz. While motion of the head and trunk were tracked during this experiment and used for previously reported analyses [10], an objective of this study is to demonstrate that the seat and back-pad measurements are sufficiently robust for monitoring postural responses, allowing us to eliminate head and trunk motion sensors. Eliminating the motion tracking system reduces analysis complexity and system costs, and makes postural assessment significantly less obtrusive.

3.2.2.2 Computers

Two personal computers were used in conducting this experiment. The first computer was used to run WCT and log task events and performance statistics. The second computer was used to collect seat and back-pad data using software created by Vista Medical Ltd. The second computer also collected position tracker data using a custom-designed LabVIEW program. Initialization of this LabVIEW program was triggered by a multi-byte signal sent via serial communication from the first computer to the second computer at the commencement of the

WCT. The synchronized initialization of the programs allowed us to calculate the difference in the two computers' internal clock times. This allowed us to synchronize seat and back-pad data with WCT data, both of which logged their computer's respective internal clock time.

3.2.2.3 Workstation Environment

In addition to the postural assessment chair, the workstation at which subjects performed the task consisted of a stand supporting a 15.0 in LCD monitor used for task presentation, and a standard keyboard and mouse/mouse pad for task interaction. Subjects were given the option to adjust stand height, seat position, and screen tilt angle to achieve their most natural working seated posture.

The room in which testing took place contained only the workstation and data collection hardware. Experimenters left the room immediately after commencement of each WCT trial and were able to observe the subject through a window from the adjacent laboratory. This was done to avoid distracting subject while he/she performed the WCT. Subjects wore headphones to hear all sounds produced by with the computer task and to block out extraneous noise created by the room's heating and cooling system, computer fans, etc.

3.3 DATA ANALYSIS

3.3.1 Data Conditioning

As mentioned, each testing trial consisted of 12 distinct 75.0 sec waves of incoming planes. After certain trials were eliminated due to equipment malfunction and data synchronization errors, data was collected during a total of 420 waves. For analysis purposes, each of the waves within a trial were examined as individual units. Waves were characterized based on (1) *wave type*, (2) *wave occurrence*, (3) *trial order*, and (4) *trial type* (Table 2).

Table 2. Conditions that characterize each wave of incoming tracks.

1. <i>Wave Type</i>	The maximum number of tracks presented within a wave (6, 12, 18, or 24 tracks)
2. <i>Wave Occurrence</i>	The first, second, or third occurrence of a particular <i>wave type</i> within a trial
3. <i>Trial Order</i>	The order in which the trial was presented (trial J is first, trial K is presented second, and trial L is presented third)
4. <i>Trial Type</i>	A wave with a low percentage of 'unidentified' tracks (trials J or L) or a high percentage of 'unidentified' tracks (trial K)

Within each wave, all calculated values and task performance statistics were linearly interpolated to match the median sample rate of the pressure mapping system, 4.57 Hz. Discrete task performance measures (e.g. Tracks on Screen, Wave Number) were rounded to the nearest whole number at each data point following interpolation. Interpolating the data allowed us to evaluate task performance and postural changes at common time points within a wave across all subjects and wave conditions.

3.3.2 Raw Posture Variables

Although all calculations and analyses presented here were performed after the data had been collected, it is our intention to employ calculations that are optimal for real-time analysis. This will aid in our ability to eventually integrate our system into an operational environment. Ten raw posture variables that are based on the pressure distribution matrix output by the pressure sensing pads were calculated at every time point throughout each wave (Table 3). Collectively, these measures of posture allow us to monitor a large range of motions with a high level of resolution over the entire scale.

Table 3. Raw Posture Variables

1. Seat Center of Pressure, Anterior/Posterior
2. Seat Center of Pressure, Medial/Lateral
3. Back Center of Pressure, Superior/Inferior
4. Back Center of Pressure, Medial/Lateral
5. Base of Support
6. Sin (Seat Yaw)
7. Root Mean Square of Seat Pressure
8. Root Mean Square of Back Pressure
9. Total Back Pressure
10. Total Pressure Ratio

Centers of Pressure (COPs) of the seat pad/buttock interface and back-pad/back interface were calculated based on a weighted average technique (Equation 1, Equation 2). This method was chosen because it requires minimal processing power, allowing for optimal temporal resolution in real-time analysis.

$$COP_y(\tau) = \frac{\sum_{i=1}^{16} \left(i \cdot \sum_{j=1}^{16} M(R_j, C_i, \tau) \right)}{\sum_{i=1}^{16} \sum_{j=1}^{16} M(R_j, C_i, \tau)}$$

Equation 1

$$COP_x(\tau) = \frac{\sum_{i=1}^{16} \left(i \cdot \sum_{j=1}^{16} M(R_i, C_j, \tau) \right)}{\sum_{i=1}^{16} \sum_{j=1}^{16} M(R_i, C_j, \tau)}$$

Equation 2

The seat pad pressure distribution matrices are oriented so that anterior/posterior movements occur in the x -direction and medial/lateral movements occur in the y -direction (Figure 5). The back-pad pressure distribution matrices are oriented so that medial/lateral movements occur in the x -direction and superior/inferior movements occur in the y -direction. The positions of the left and right ischial tuberosities were approximated as the $COPs$ of the left and right halves of the seat pad pressure matrix (*Equation 3, Equation 4, Equation 5, Equation 6*).

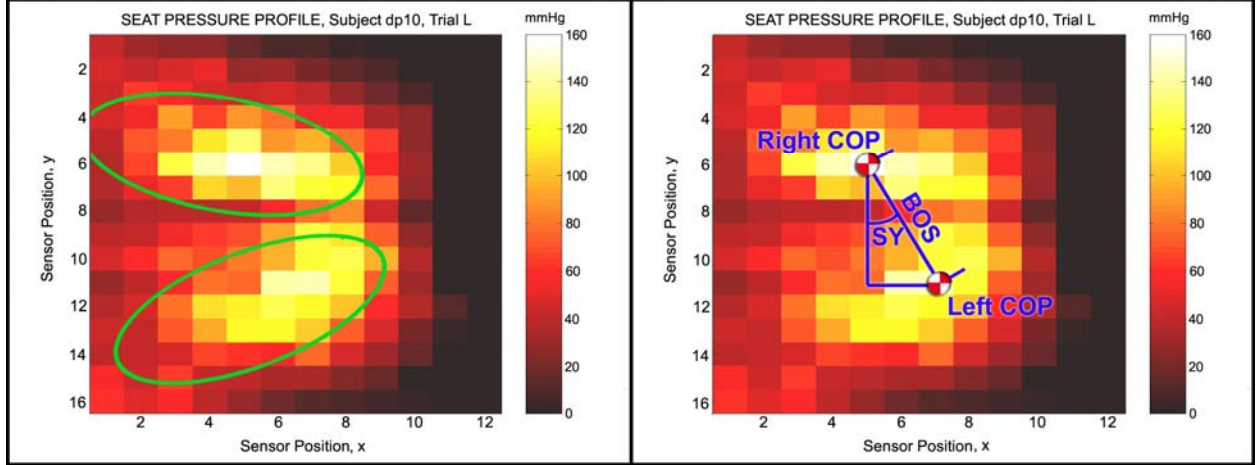


Figure 5. Left: Seat pressure profile with overlay (green) to highlight the location of the left and right posterior thigh and buttock. The subject is oriented so that $x = 0$ corresponds to the front edge of the seat. Right: Seat pressure profile with overlay highlighting Left Center of Pressure (Left COP), Right Center of Pressure (Right COP), Base of Support (BOS), and Seat Yaw Angle (SY).

$$COP_{Left,y}(\tau) = \frac{\sum_{i=1}^8 \left(i \cdot \sum_{j=1}^{16} M(R_j, C_i, \tau) \right)}{\sum_{i=1}^8 \sum_{j=1}^{16} M(R_j, C_i, \tau)}$$

Equation 3

$$COP_{Left,x}(\tau) = \frac{\sum_{i=1}^{16} \left(i \cdot \sum_{j=1}^8 M(R_j, C_i, \tau) \right)}{\sum_{i=1}^{16} \sum_{j=1}^8 M(R_j, C_i, \tau)}$$

Equation 4

$$COP(\tau)_{Right,y} = \frac{\sum_{i=9}^{16} \left(i \cdot \sum_{j=1}^{16} M(R_j, C_i, \tau) \right)}{\sum_{i=9}^{16} \sum_{j=1}^{16} M(R_j, C_i, \tau)}$$

Equation 5

$$COP_{Right,x}(\tau) = \frac{\sum_{i=1}^{16} \left(i \cdot \sum_{j=9}^{16} M(R_j, C_i, \tau) \right)}{\sum_{i=1}^{16} \sum_{j=9}^{16} M(R_j, C_i, \tau)}$$

Equation 6

Once the position of the left and right centers of pressure had been calculated, the seated base of support (*BOS*) was calculated as the length of the vector connecting them (*Equation 7*) (Figure 5). It is often noted in standing literature that widening the standing BOS (distance between the feet) ensures more stable balance. Seated subjects are capable of altering their seated BOS by internally and externally rotating the femur about the hip. The left and right centers of pressure were also used to monitor changes in subjects' orientation in the transverse plane. To do so, the sine of the angle between the vector connecting the left and right ischial tuberosities and the front edge of the seat was calculated. This variable is termed sine of seat yaw (*SSY*) (*Equation 8*) (Figure 5).

$$BOS(\tau) = \sqrt{(COP_{Right,y}(\tau) - COP_{Left,y}(\tau))^2 + (COP_{Right,x}(\tau) - COP_{Left,x}(\tau))^2}$$

Equation 7

$$SSY(\tau) = \sin\left(\tan^{-1}\left(\frac{COP_{Right,y}(\tau) - COP_{Left,y}(\tau)}{COP_{Right,x}(\tau) - COP_{Left,x}(\tau)}\right)\right)$$

Equation 8

The root mean square of the seat pressure and the root mean square of the back pressure provide a relative measure of a general increase or decrease in movement. This variable is calculated as the standard deviation of the instantaneous first order derivative of pressure at each pressure sensor in either pad. At a given time point during the wave for a given sensor, the instantaneous first order derivative of pressure is calculated as the slope of first order polynomial fit to the pressure recorded by the sensor within a 1.10 sec (5 data points) window.

Two variables were calculated to monitor how subjects braced their backs against the back of the chair. Total back pressure was calculated as the sum of pressures recorded at each of the 256 pressure sensors imbedded in the back mat. The total pressure ratio was calculated as the ratio of the total back pressure to the sum of the total back and seat pressure.

3.3.3 Gross Postural Changes

To gauge how general tendencies in seated posture varied across wave conditions, certain measures were calculated to quantify movement throughout an entire wave. Such measures are commonly reported in standing dual task paradigm literature. Summing the distance traveled by the seat surface *COP* between sequential time points throughout the wave provides an estimate of total movement, ΔCOP (Equation 9).

$$\Delta COP = \sum_{\tau=2}^{\tau=343} \sqrt{(COP_y(\tau) - COP_y(\tau-1))^2 + (COP_x(\tau) - COP_x(\tau-1))^2}$$

Equation 9

In addition, the total change in base of support, ΔBOS , was calculated by summing the absolute change in *BOS* between sequential time points throughout the wave (Equation 10), and the total change in seat yaw, ΔSY , was calculated by summing the absolute change in seat yaw angle between sequential time points throughout the wave (Equation 11).

$$\Delta BOS = \sum_{\tau=2}^{\tau=343} |BOS(\tau) - BOS(\tau-1)|$$

Equation 10

$$\Delta SY = \sum_{\tau=2}^{\tau=343} |SY(\tau) - SY(\tau - 1)|$$

Equation 11

3.3.4 Level of Engagement

3.3.4.1 Posture-Task Correlation

An objective of this study was to identify instances throughout the course of the task when posture was affected by changing task conditions. In order to identify these instances, it was determined how each of the ten posture variables (Table 3) were correlated to the number of tracks on the screen within a moving window of time. From data points $\tau = 21$ to $\tau = T-20$ of each wave, the correlation between tracks on screen (t) and each of the posture variables (V_i) was calculated within a 9.0 sec (± 20 data points) window centered at the given data point (*Equation 12*) (Figure 6). This correlation was referred to as the level of ‘postural engagement’.

$$r_i(\tau) = \frac{\sum_{p=\tau-20}^{\tau+20} \left(\left(V_i(p) - \frac{\sum_{q=\tau-20}^{\tau+20} V_i(q)}{41} \right) \cdot \left(t(p) - \frac{\sum_{q=\tau-20}^{\tau+20} t(q)}{41} \right) \right)}{\sqrt{\sum_{p=\tau-20}^{\tau+20} \left(V_i(p) - \frac{\sum_{q=\tau-20}^{\tau+20} V_i(q)}{41} \right)^2 \cdot \sum_{p=\tau-20}^{\tau+20} \left(t(p) - \frac{\sum_{q=\tau-20}^{\tau+20} t(q)}{41} \right)^2}}$$

Equation 12

Squaring the correlation coefficient that was calculated at each time point yielded the percentage of the observed variance within the window described by the relationship between the posture variable and number of tracks on screen. The term ‘high postural engagement’ was used to describe instances in which a posture variable was highly correlated to the number of tracks on screen ($r_i(\tau)^2 \geq 0.50$) within the window.

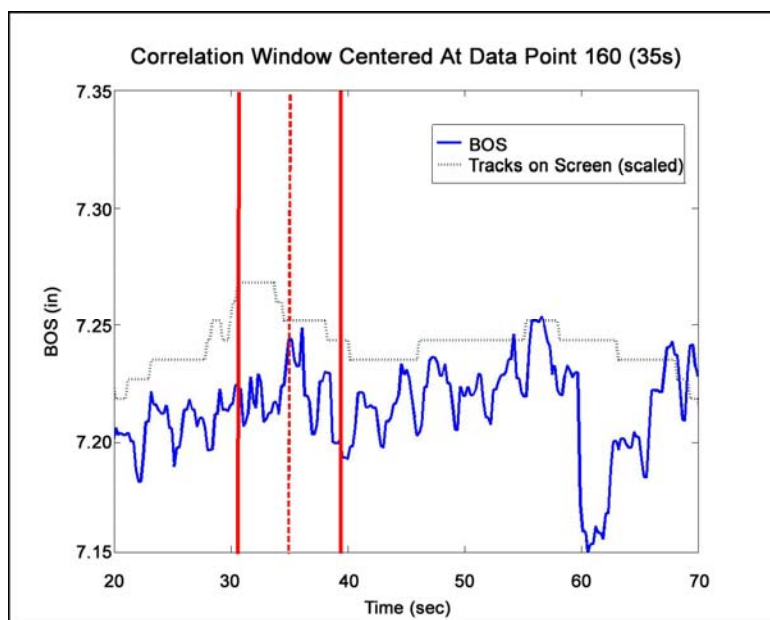


Figure 6. Example of the moving correlation window. Here, the base of support (BOS) is being correlated with the instantaneous number of tracks on screen in a window centered at data point 160 (35 sec) as is indicated by the dashed red line. The solid red lines indicate the upper and lower temporal boundaries of the window, which spans ± 20 data points.

The cumulative relationship of the postural measures that are highly correlated to the contexts of the task was then used to construct the implicit gauge of cognitive state. At each point in a wave it was determined how many of the ten posture variables were highly correlated with the number of tracks on screen within the moving window (*Equation 13*). This was termed the ‘cumulative postural engagement response’, $N(\tau)$.

$$N(\tau) = \sum_{i=1}^{10} n_i(\tau) \begin{cases} = 1, & r_i^2 \geq 0.50 \\ = 0, & r_i^2 < 0.50 \end{cases}$$

Equation 13

As will be discussed below, $N(\tau)$ appears to be dependent on the contexts of the task (i.e. the time course of the number of tracks on screen). Thus, it is hypothesized based on deductive reasoning that the task contexts can be predicted by first predicting the number of highly correlated variables at a given data point. To do so, a mathematical classifier was trained to predict $N(\tau)$ based on the values of the posture variables at data point τ as well as their values at points prior to data point τ .

3.3.4.2 Multivariate Discriminant Analysis

Multiple variables measured at a given data point can be used to define a single observation at that data point. Due to the way in which these defining variables co-vary, it is often evident that observations made from within the same data set can be segregated into multiple groups. Observations belonging to a particular grouping will typically share some common

characterization that distinguish them from observations belonging to a different group. Figure 7 provides a generic demonstration of observations defined by the same two variables that clearly can be segregated into two groups.

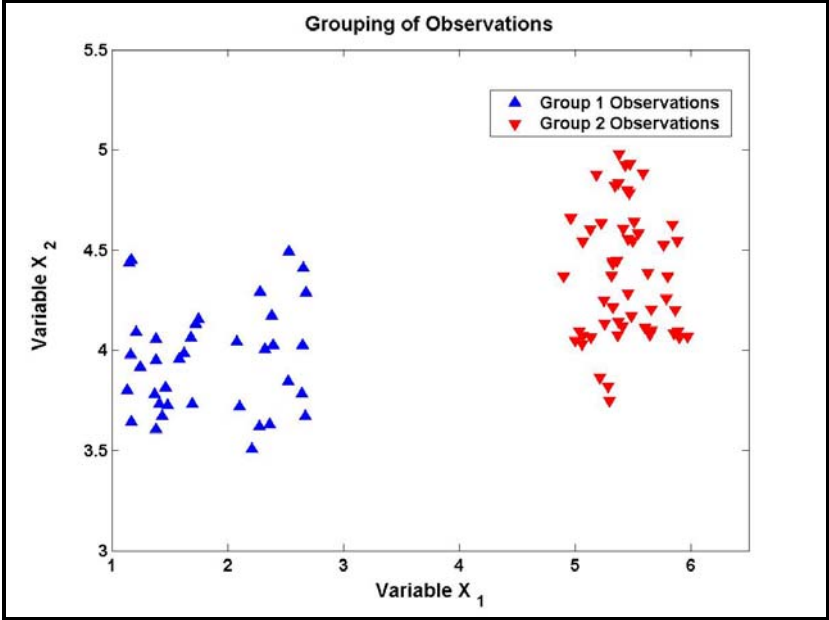


Figure 7. Observation from within the same data set may be segregated into distinct groups.

Mathematical classifiers are used to segregate observations made from one data set into specific groups of observations. Using a priori knowledge of (a) the probability of any observation belonging to a particular group and/or (b) the mean values of the variables which define the observations that belong to a particular group, classifiers are trained to assign unclassified observations to groups by mathematically manipulating the variables that define them (Figure 8).

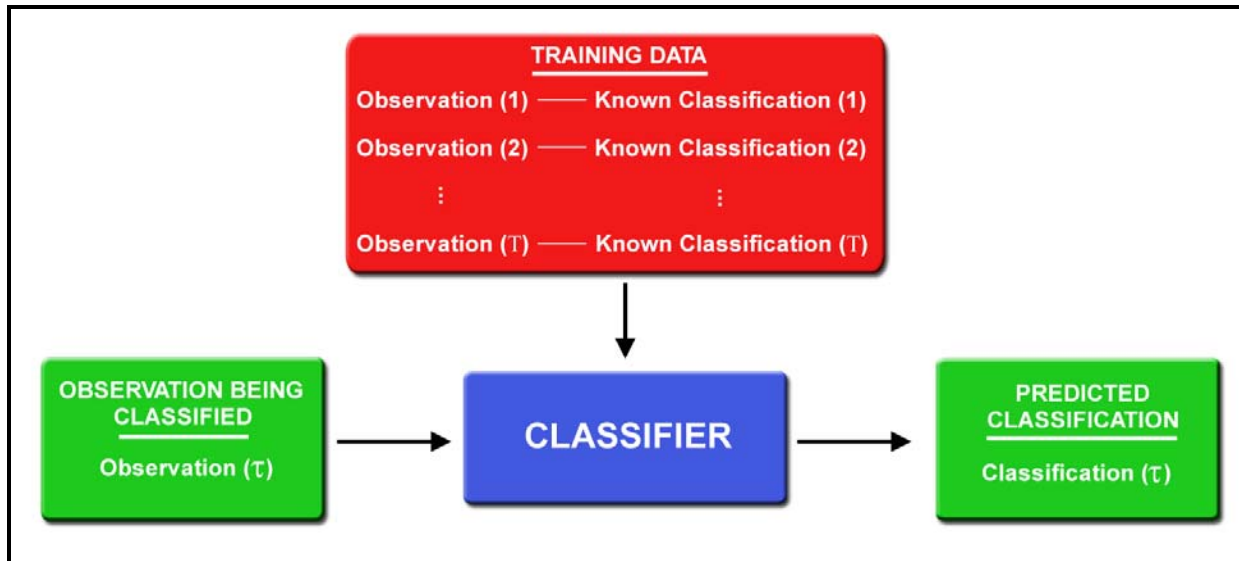


Figure 8. Basic model of a multivariate classifier. The classifier is trained to classify an observation based on the relationship between the training observations (defined by a collection of variables) and their known classifications.

The current study aims to determine whether observations, which were defined by a collection of posture variables, could be classified into groups with common values of $N(\tau)$. An observation made at data point τ is represented by the matrix $X(\tau)$. This matrix is defined by n number of posture variables calculated at data point τ (Equation 14). These posture variables consist of the ten posture variables defined in Table 3 ($V(\tau)$) calculated at point τ and at points prior to τ . For example $V(\tau)$, $V(\tau-16)$, and $V(\tau-32)$ may all be used in defining $X(\tau)$.

$$X(\tau) = [\chi_1 \ \chi_2 \ \dots \ \chi_n]$$

Equation 14

As previously mentioned, a set of training observations with known classifications is needed to train the classifier. The current study is more concerned with demonstrating that the observations (with already known classification) can be grouped according to $N(\tau)$ than it is concerned with predicting the classification of unclassified observations. Therefore, the classifier was used to reclassify the training data (Figure 9). The observations were considered distinctly grouped if the classifier could reclassify the observations, thus correctly predicting $N(\tau)$, with a high degree of accuracy.

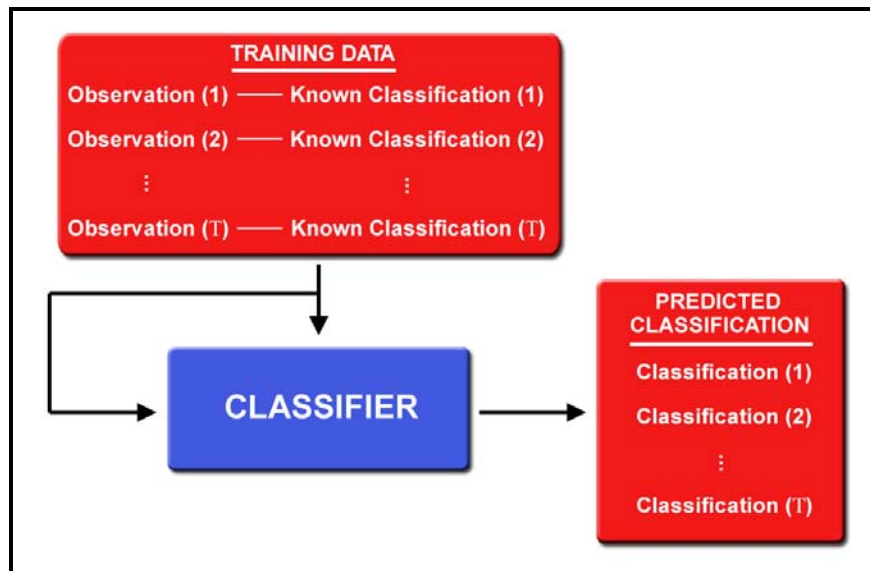


Figure 9. Use of classifier in the current study. A mathematical classifier was used to reproduce the known classifications of the training observations.

To train the classifier, all observations made during every wave were manually grouped according to their respective values of $N(\tau)$. The matrix X_g consists those observation that belong to a particular group g . As an example, consider that we are attempting to classify observations into three groups: group X_1 (observations made at data points where $N(\tau) = 1, 2,$ or

3); group X_2 (observations made at data points where $N(\tau) = 4, 5, \text{ or } 6$); or X_3 (observations made at data points where $N(\tau) = 7, 8, 9, \text{ or } 10$). As was the case in defining individual observations, these groups of observations are defined by subgroups of posture variables (*Equation 15*).

$$X_g = [\chi_{1,g} \ \chi_{2,g} \ \dots \ \chi_{n,g}]$$

Equation 15

Once the training variables had been manually grouped, a Mahalanobis distance classification algorithm was used reclassify the observations. The Mahalanobis distance, D , between two observations (each defined by n number of variables) is a measure of the spatial distance that separates them in n dimensional space. This means of measuring the distance between points varies from the Euclidian distance in that it incorporates the training data set covariance matrix, S , to account for the differential variances and correlations between the variables. In order to classify an observation, the Mahalanobis distance between the observation and the mean observation values of each group was calculated (*Equation 16, Equation 17*) [35]. The observation was classified as belonging to the group whose mean value observation was the smallest Mahalanobis distance away.

$$\bar{X}_g = [\bar{\chi}_{1,g} \ \bar{\chi}_{2,g} \ \dots \ \bar{\chi}_{n,g}]$$

Equation 16

$$D = \sqrt{(\mathbf{X}(\tau) - \bar{\mathbf{X}}_g)^T \mathbf{S}^{-1} (\mathbf{X}(\tau) - \bar{\mathbf{X}}_g)}$$

Equation 17

3.3.4.3 Principal Component Analysis

After it had been demonstrated that $N(\tau)$ can be satisfactorily predicted via the classification method explained in section 3.3.4.2, principal component analysis was used to (a) determine the degree to which the posture variables are independent from each other and (b) remove random variability from the data, which can subsequently reduce the dimensionality required to predict the cumulative postural engagement response. Principal component analysis essentially provides a means of transforming a set of correlated variables into a new set of uncorrelated variables [24]. The following paragraphs provide a general summary of the objectives and advantages of this analysis and methods by which it was performed.

Again, each observation was characterized by the combination of n posture variables making up $\mathbf{X}(\tau)$. Imagine the variables defining every observation $\mathbf{X}(\tau)$ being plotted in a coordinate system consisting of n orthogonal axes. Each of these axes represents one of the n number of variables. A new axis, or the first principal component, can be defined in such a way that it accounts for the maximum amount of the data's variance in n -dimensional space. A second axis, or the second principal component, is defined so that it accounted for the data's maximum amount of variance while being orthogonal to the first principal component (Figure 10). This process continues so that n principal components are defined. Just as each axis of the original coordinate system represents one of the posture variables ($\chi_1, \chi_2, \dots, \chi_n$), each of the principal components represents a new variable (u_1, u_2, \dots, u_n). The advantage to redefining the

data in the principal component coordinate system is that the variance defined by each of the new variables is not redundant. Therefore, the principal components are completely independent.

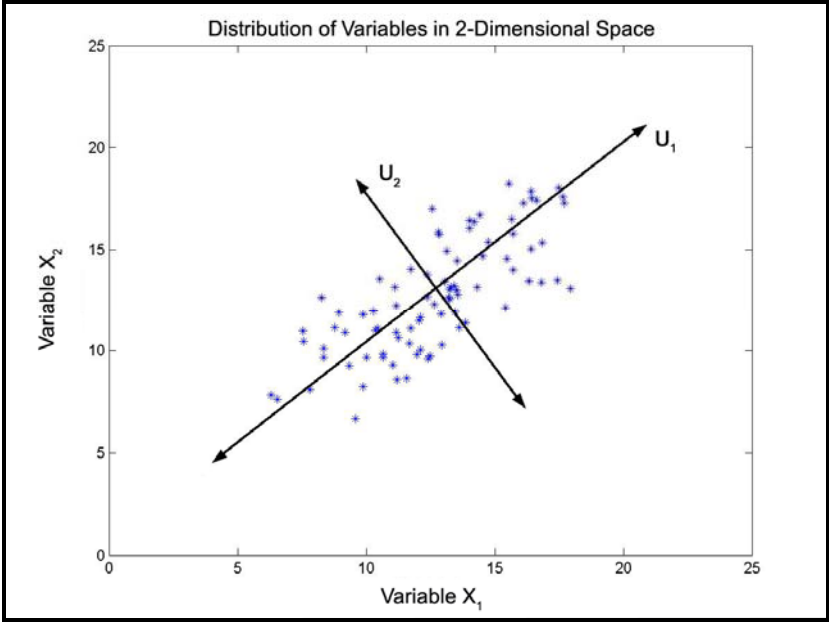


Figure 10. Two-variable principal component example. Variables X_1 and X_2 define 85 observations. A second coordinate system is defined in which the first principal component, U_1 , accounts for the maximum amount of data's variance. The second principal component, U_2 , is orthogonal to U_1 . U_1 accounts for 87.5% of the data's total variance, and U_2 accounts for 12.5% of the data's total variance.

Since the original coordinate system and the principal component coordinate system are both n -dimensional and orthogonal, the relationship between the two is mathematically defined in terms of a simple rotation matrix, \mathbf{R} (Equation 18).

$$[u_1 \ u_2 \ \dots \ u_n] = \begin{bmatrix} R_{11} & R_{12} & \dots & R_{1n} \\ R_{21} & R_{22} & \dots & R_{2n} \\ \dots & \dots & \dots & \dots \\ R_{n1} & R_{n2} & \dots & R_{nn} \end{bmatrix} \times [\chi_1 \ \chi_2 \ \dots \ \chi_n]^T$$

Equation 18

The total variance of the data accounted for by a given principal component is equal to the respective eigenvalue of the covariance matrix of \mathbf{X} . In general, when the original variables are highly dependent the first few principal components will account for the majority of the data's variance. However, when the original variables are highly independent, each eigenvalue of the covariance matrix will be relatively equal, and thus each principal component will equally account for the data's variance. The principal components that account for little of the data's variance do not substantially enhance the ability to define a linear combination of principal components that can be used to reproduce the observations. These components can therefore be disregarded to reduce dimensionality and simplify the discriminant analysis.

Equation 18 shows that each principal component can be defined as a weighted sum of the original variables. Analyzing the weights, or coefficients, associated with each original variable making up a principal component helps describe the degree to which each original variable contributes to the total variance of the data. For instance, if the original variables were highly dependent on each other and the absolute values of coefficients associated with a given variable were relatively low except in the definition of the last principal component, it would be concluded that the variable contributes little to the total variance. However, if the original variables were highly uncorrelated and each variable was associated with at least one coefficient

with a relatively high absolute value, it would be concluded that each variable contributes to the total variance considerably.

After the principal components had been defined, an arbitrarily-chosen cutoff was set to decide which principal components accounted for a considerable amount of the data's total variance (80%). The rotation matrix \mathbf{R} in *Equation 18* was truncated so that only those necessary principal components would be computed, and each $\mathbf{X}(\tau)$ was then transformed to principal component terms, $\mathbf{U}(\tau)$. Each observation was redefined using the principal component variables and was then reclassified using the Mahalanobis distance classification technique explained in section 3.3.4.2. This was performed to determine if the observations could be classified with reduced dimensionality but without substantial loss of prediction power.

3.3.5 Statistical Analysis

It was determined whether or not each wave condition (*wave type*, *wave occurrence*, *trial order*, and *trial type*) significantly affected the gross postural changes during a wave (ΔCOP , ΔBOS , and ΔSY). Analysis of variance was performed to determine if each wave condition significantly affected each measurement of change in posture. However, upon analyzing the distribution of the fitted model residuals with the Shapiro-Wilk test, it was found that the normality assumption necessary for using the analysis of variance was not valid.

Therefore, the effects of the wave conditions on gross postural changes were analyzed using analysis of variance of the log-transformed data, which was more normally distributed. The log-transformed data was also used to investigate the interaction effects of the wave conditions via analysis of variance. All post-hoc analyses were performed using Tukey's HSD post-hoc test.

It was also tested whether or not the cumulative posture engagement response, $N(\tau)$, varied with task difficulty. At various common time points throughout each wave, ANOVA was used to test the effect of the condition *wave type* on $N(\tau)$. Again, post-hoc analysis was performed using Tukey's HSD post-hoc test.

4.0 RESULTS

4.1 GROSS POSTURAL CHANGES

Seat COP stabilograms provide a qualitative means of investigating the correlation of dynamic seated posture and cognitive task difficulty. Visual analysis of stabilograms plotted for different *wave types* supports the hypothesis that changes in seated posture may be dependent on the task conditions that vary with the number of tracks on screen. Figure 11 provides an example of a subject's seat COP path changing as the number of tracks on screen increases. It can be seen here that the total area traveled by the COP decreased during the wave with 24 maximum tracks, and postural shifts appear to be less sporadic.

To quantitatively investigate these findings, gross postural changes over an entire wave were measured as ΔCOP , ΔBOS , and ΔSY . On average throughout a wave, the seated center of pressure traveled a distance of 5.51 in (ΔCOP), the distance between the left and right ischial tuberosities changed 2.61 in (ΔBOS), and the pelvis rotated 0.43 rad in the transverse plane (ΔSY) (Table 4).

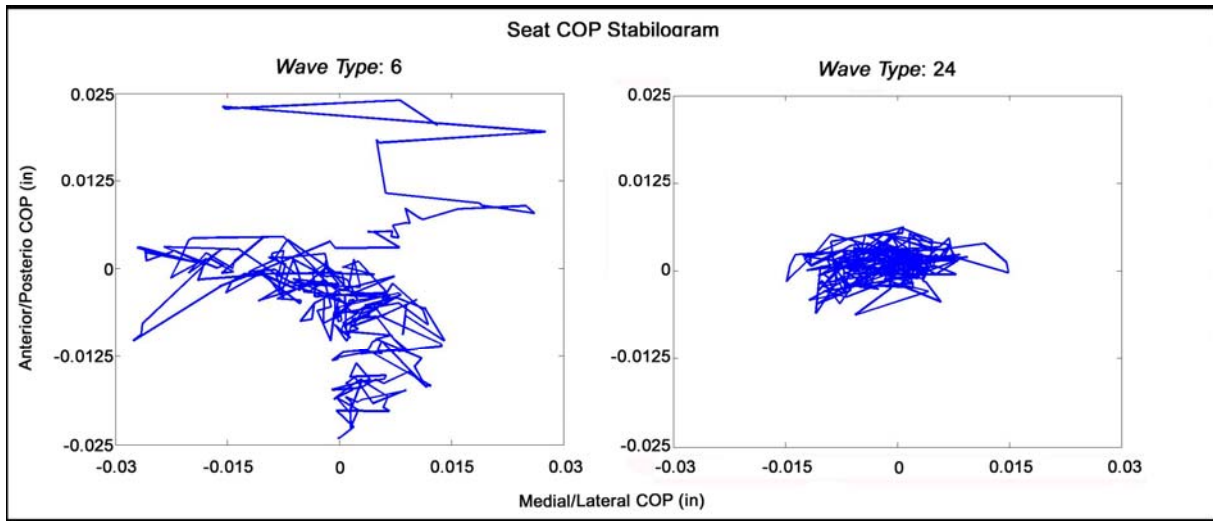


Figure 11. Stabilograms depicting how a subject’s seated posture varies while completing waves with a maximum of 6 (left) and 24 tracks (right).

Table 4. Summary of gross postural changes over all waves (n = 420).

	ΔCOP (in)	ΔBOS (in)	ΔSY (rad)
Minimum	0.71	0.48	0.06
Maximum	24.98	16.90	1.52
Mean	5.51	2.61	0.43

The probability of each wave condition (*wave type*, *wave occurrence*, *trial order*, and *trial type*) having a significant effect on these measures was quantified by performing an analysis of variance using the log-transform of each measure ($\log(\Delta COP)$, $\log(\Delta BOS)$, and $\log(\Delta SY)$). All three measures of gross postural change were significantly affected by the condition *wave type* ($p < 0.0001$). As is shown in Figure 12, Figure 13, and Figure 14, there was a general decrease in postural movement as task difficulty (i.e. the total number of tracks on screen) increased. The average values of $\log(\Delta COP)$, $\log(\Delta BOS)$, and $\log(\Delta SY)$ decreased as the maximum number of

tracks on screen increased from 6 to 12 tracks and from 12 to 18 tracks. The average value of each measure then increased as the maximum number of tracks on screen increased from 18 to 24 tracks. Post-hoc tests were performed to determine specifically which *wave types* significantly effected the gross postural measures. $\log(\Delta COP)$, $\log(\Delta BOS)$, and $\log(\Delta SY)$ were all significantly higher during waves of 6 maximum tracks than waves of 18 or 24 maximum tracks. $\log(\Delta COP)$, $\log(\Delta BOS)$, and $\log(\Delta SY)$ were also significantly higher during waves of 12 maximum tracks than waves of 18 maximum tracks.

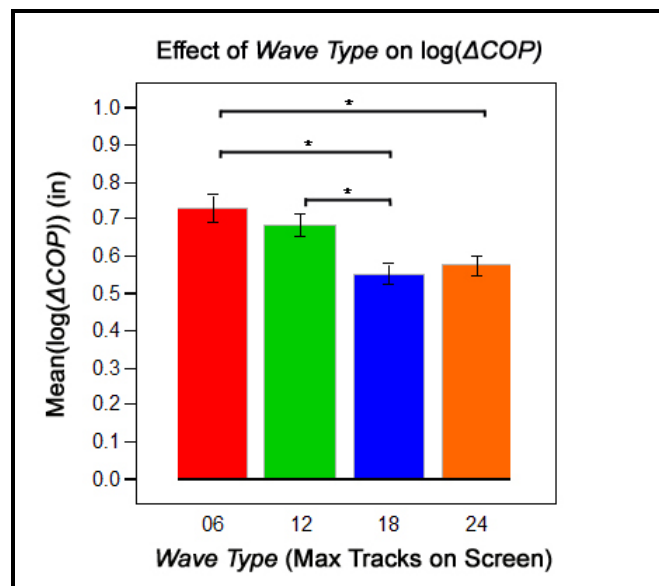


Figure 12. The difficulty of the task significantly affects the total distance traveled by the center of pressure $\log(\Delta COP)$. Standard error bars included. (* significant difference, $p < 0.05$)

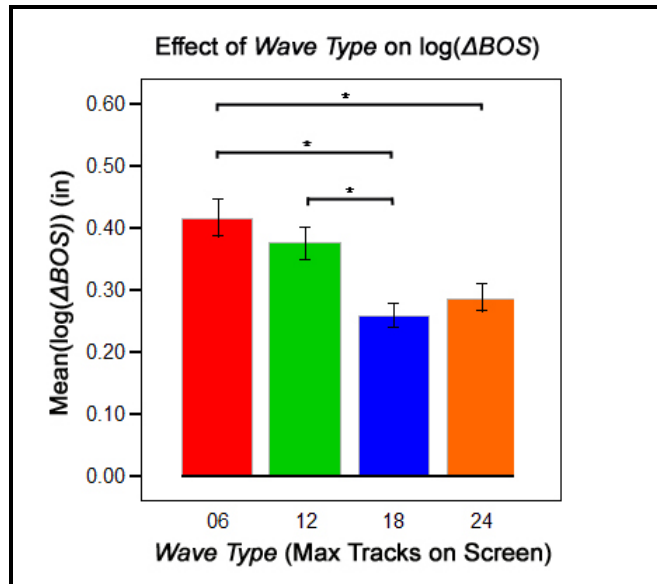


Figure 13. The difficulty of the task significantly affects the total change in base of support (ΔBOS). Standard error bars included. (* significant difference, $p < 0.05$)

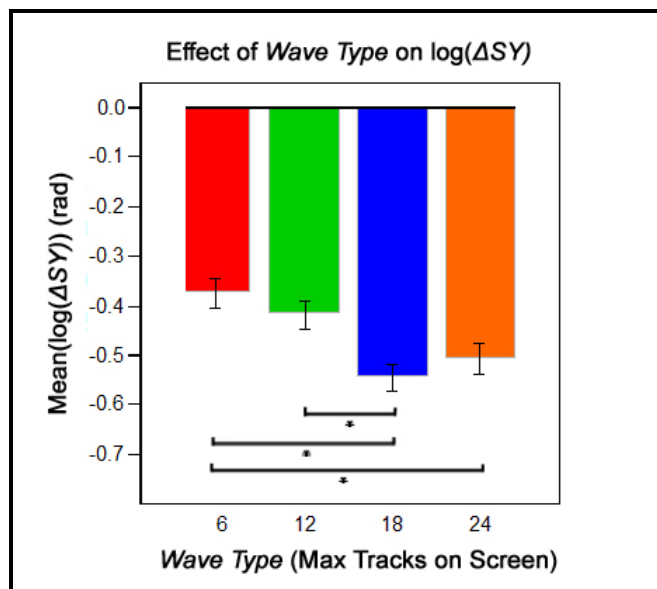


Figure 14. The difficulty of the task significantly affects the total change in seat yaw (ΔSY). Standard error bars included. (* significant difference, $p < 0.05$)

None of the other wave conditions (*trial order*, *trial type*, and *wave occurrence*) significantly affected $\log(\Delta COP)$, $\log(\Delta BOS)$, or $\log(\Delta SY)$. Because these conditions defined waves in conjunction with *wave type*, which was found to significantly affect gross postural changes, the interaction effects of *trial order* x *wave type*, *trial order* x *wave type*, and *trial order* x *wave type* were analyzed. However, none of these interaction effects were significant. Thus, *wave type* was the only wave condition that significantly affected gross postural changes.

4.2 POSTURAL ENGAGEMENT RESULTS

4.2.1 Changes in Postural Engagement

As previously mentioned, the level of postural engagement is the degree to which changes in a given posture variable and changes in the instantaneous number of tracks on screen are correlated within a moving window of time. Figure 15 provides a simple example of postural engagement varying as the contexts of the task (i.e. tracks on screen) change.

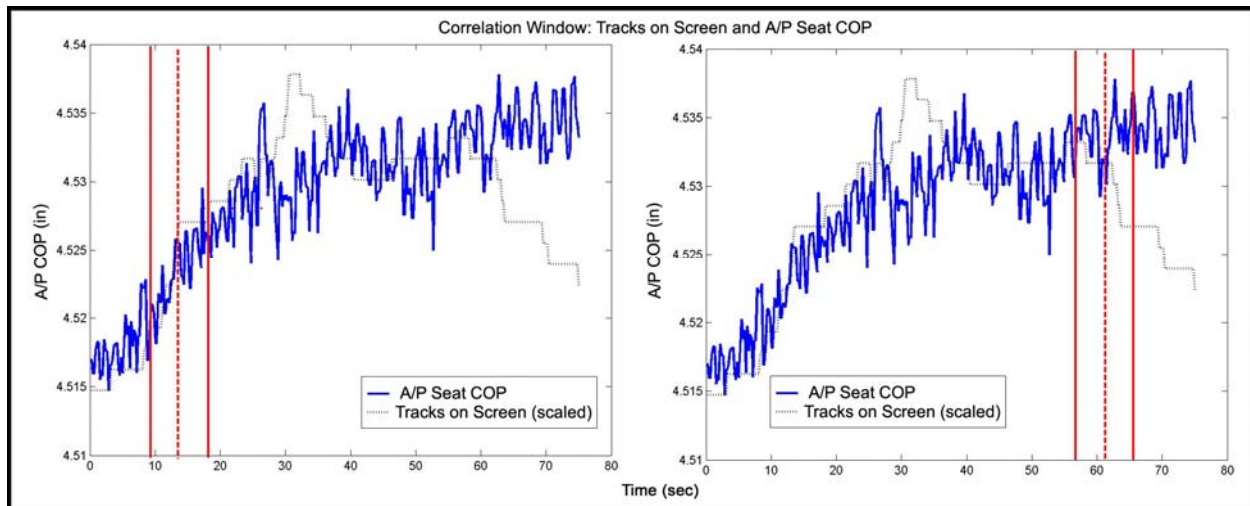


Figure 15. Examples of the moving correlation window during a wave of 18 tracks. The left graph illustrates a region of high correlation. Within the window centered at 13.1 sec (data point 60), anterior/posterior seat center of pressure is correlated with tracks on screen with a correlation coefficient of $r = 0.82$. The right graph illustrates a region of low correlation. Within the window centered at 61.3 sec (data point 280), anterior/posterior seat center of pressure is correlated with tracks on screen with a correlation coefficient of $r = 0.20$.

The number of posture variables that are highly correlated to tracks on screen at a given data point is referred to as the cumulative postural engagement, $N(\tau)$. Plotting $N(\tau)$ at each data point averaged over all 420 waves helps to show the dynamic nature of the cumulative postural engagement response, \bar{N} (Figure 16).

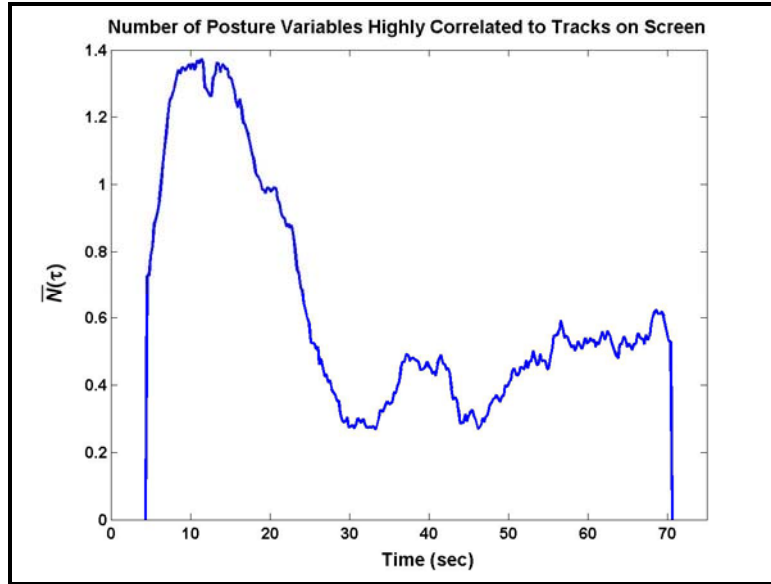


Figure 16. Average cumulative postural engagement response, \bar{N} . The average number of posture variables that are highly correlated to tracks on screen is a very dynamic measure of postural engagement.

To demonstrate how this pattern changes with respect to the contexts of the task, $\bar{N}(\tau)$ was recalculated for each value of the wave condition *wave type* ($\bar{N}_6(\tau)$, $\bar{N}_{12}(\tau)$, $\bar{N}_{18}(\tau)$, $\bar{N}_{24}(\tau)$) and plotted with the respective average instantaneous number of tracks on screen ($\bar{i}_6(\tau)$, $\bar{i}_{12}(\tau)$, $\bar{i}_{18}(\tau)$, $\bar{i}_{24}(\tau)$) (Figure 17).

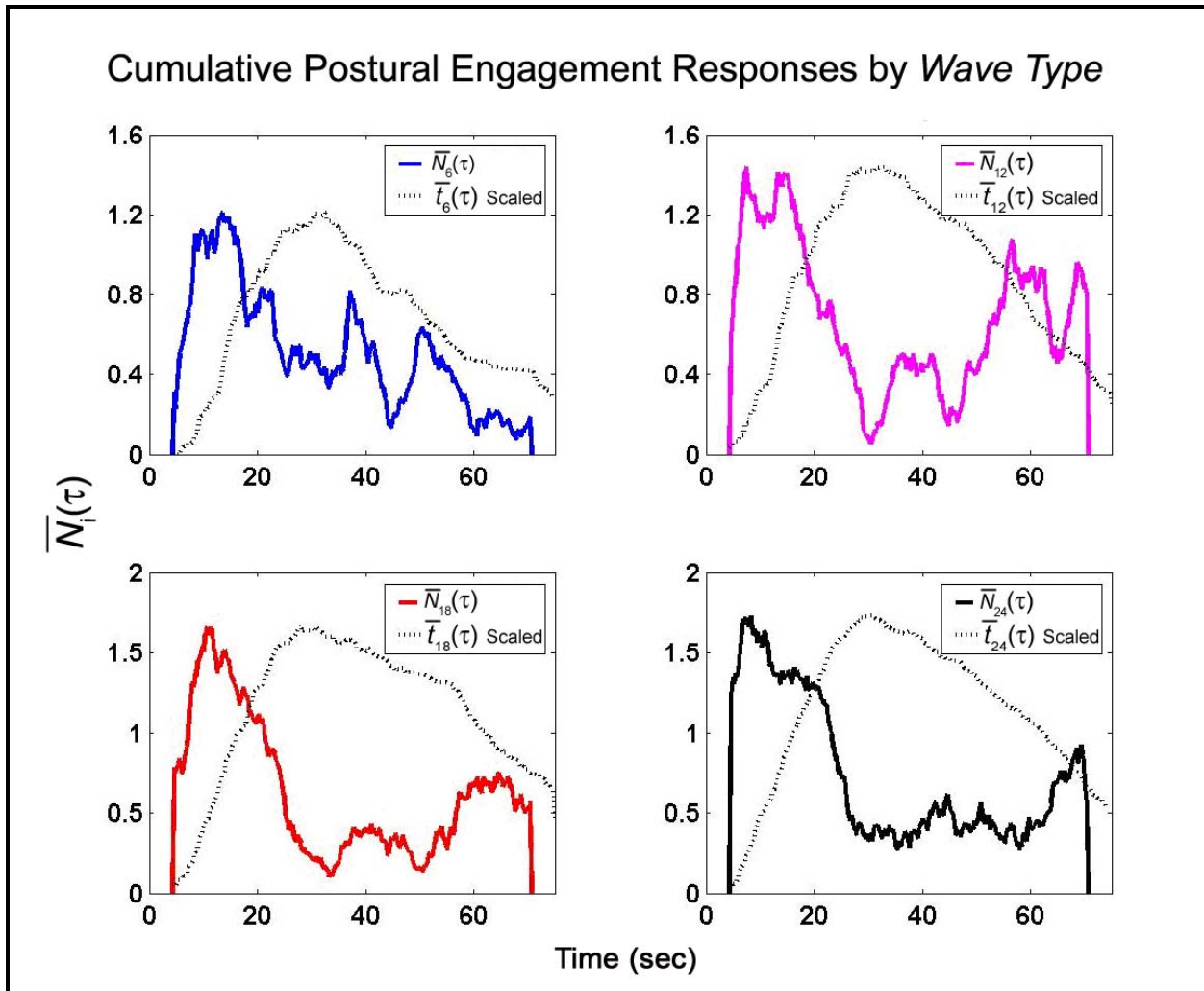


Figure 17. $\bar{N}_6(\tau)$ (top left), $\bar{N}_{12}(\tau)$ (top right), $\bar{N}_{18}(\tau)$ (bottom left), and $\bar{N}_{24}(\tau)$ (bottom right) are plotted with rescaled values of $\bar{t}_6(\tau)$, $\bar{t}_{12}(\tau)$, $\bar{t}_{18}(\tau)$, and $\bar{t}_{24}(\tau)$ respectively. In each case, the maximum value of $\bar{N}_i(\tau)$ occurred during the initial buildup of tracks on screen, followed by a sudden decrease in $\bar{N}_i(\tau)$ prior to tracks on screen reaching its maximum value. Note that $\bar{N}_6(\tau)$ did not increase towards the end of the wave as the other value of $\bar{N}_i(\tau)$ did.

Patterns of postural engagement are generally consistent regardless of *wave type*. In each case, $\bar{N}_i(\tau)$ reached its maximum value during the initial buildup of tracks on screen. $\bar{N}_i(\tau)$ then decreased prior to the number of tracks on screen reaching its maximum value. However, $\bar{N}_6(\tau)$, $\bar{N}_{12}(\tau)$, $\bar{N}_{18}(\tau)$, and $\bar{N}_{24}(\tau)$ are obviously not identical. The most distinct difference amongst the average measures of cumulative postural engagement response occurs at the end of a wave. While $\bar{N}_6(\tau)$ generally continued to decrease with the number of tracks on screen, $\bar{N}_{12}(\tau)$, $\bar{N}_{18}(\tau)$, and $\bar{N}_{24}(\tau)$ all began to increase at approximately 50-55 sec, while the wave was nearing its end.

More subtle differences between the average measures of cumulative postural engagement become apparent by plotting $\bar{N}_6(\tau)$, $\bar{N}_{12}(\tau)$, $\bar{N}_{18}(\tau)$, and $\bar{N}_{24}(\tau)$ together against time (Figure 18).

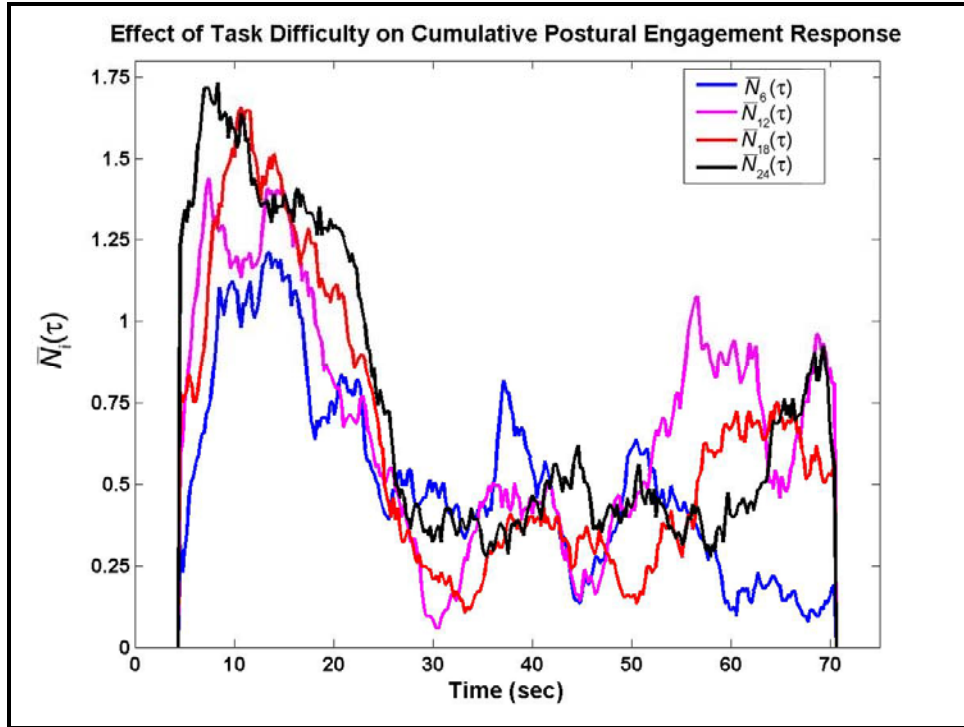


Figure 18. The average number of highly correlated variables varies with task difficulty, with distinct differences occurring up to 25s.

Towards the beginning of a wave (0-25 sec), the magnitudes of $\bar{N}_{24}(\tau)$, $\bar{N}_{18}(\tau)$, $\bar{N}_{12}(\tau)$, and $\bar{N}_6(\tau)$ were typically ordered at each point according to their respective maximum number of tracks on screen ($\bar{N}_{24}(\tau) > \bar{N}_{18}(\tau) > \bar{N}_{12}(\tau) > \bar{N}_6(\tau)$). Figure 17 shows that during this phase of the wave, new tracks were constantly being presented to the subjects, and the rate at which the tracks were presented was proportional to the maximum number of tracks on screen. Thus, greater influx of tracks on screen resulted in higher postural engagement on average. Towards the end of a wave, $\bar{N}_{24}(\tau)$, $\bar{N}_{18}(\tau)$ and $\bar{N}_{12}(\tau)$ show that subjects again exhibited higher postural engagement as the number of tracks on screen decreased. However, this trend was not found for $\bar{N}_6(\tau)$, as will be discussed below.

Using data from all 420 waves, the statistical difference between $N_6(\tau)$, $N_{12}(\tau)$, $N_{18}(\tau)$, and $N_{24}(\tau)$ was calculated at data points 21 - 322 (4.6 - 70.4 sec). Of the 301 data points analyzed, 19.9% of the points were scaled so that $\bar{N}_6(\tau) < \bar{N}_{12}(\tau) < \bar{N}_{18}(\tau) < \bar{N}_{24}(\tau)$. At 66.7% of those data points, $\bar{N}_6(\tau)$, $\bar{N}_{12}(\tau)$, $\bar{N}_{18}(\tau)$, and $\bar{N}_{24}(\tau)$ were significantly different. At 60.8% of all 301 data points, there was a significant difference between $\bar{N}_6(\tau)$, $\bar{N}_{12}(\tau)$, $\bar{N}_{18}(\tau)$, and $\bar{N}_{24}(\tau)$. Table 5 provides a summary of the statistical differences between each $\bar{N}_i(\tau)$ at 20 different data points spaced 3.3 sec apart throughout the trial.

Table 5. Differences in $n \bar{N}_6(\tau)$, $\bar{N}_{12}(\tau)$, $\bar{N}_{18}(\tau)$, and $\bar{N}_{24}(\tau)$ throughout a wave.

Data Point	Time (sec)	Relative Magnitudes	Probability of No Difference
25	5.5	$\bar{N}_6(\tau) < \bar{N}_{12}(\tau) < \bar{N}_{18}(\tau) < \bar{N}_{24}(\tau)$	<0.001
40	8.7	$\bar{N}_6(\tau) < \bar{N}_{12}(\tau) < \bar{N}_{18}(\tau) < \bar{N}_{24}(\tau)$	0.057
55	12.0	$\bar{N}_6(\tau) < \bar{N}_{12}(\tau) < \bar{N}_{24}(\tau) < \bar{N}_{18}(\tau)$	<0.05
70	15.3	$\bar{N}_6(\tau) < \bar{N}_{18}(\tau) < \bar{N}_{12}(\tau) < \bar{N}_{24}(\tau)$	0.581
85	18.6	$\bar{N}_6(\tau) < \bar{N}_{12}(\tau) < \bar{N}_{18}(\tau) < \bar{N}_{24}(\tau)$	<0.05
100	21.9	$\bar{N}_{12}(\tau) < \bar{N}_6(\tau) < \bar{N}_{18}(\tau) < \bar{N}_{24}(\tau)$	<0.05
115	25.1	$\bar{N}_6(\tau) < \bar{N}_{12}(\tau) = \bar{N}_{18}(\tau) < \bar{N}_{24}(\tau)$	0.156
130	28.4	$\bar{N}_{18}(\tau) < \bar{N}_{12}(\tau) < \bar{N}_6(\tau) < \bar{N}_{24}(\tau)$	0.239
145	31.7	$\bar{N}_{12}(\tau) < \bar{N}_{18}(\tau) < \bar{N}_6(\tau) < \bar{N}_{24}(\tau)$	<0.05
160	35.0	$\bar{N}_{18}(\tau) < \bar{N}_{24}(\tau) < \bar{N}_{12}(\tau) < \bar{N}_6(\tau)$	0.073
175	38.3	$\bar{N}_{24}(\tau) < \bar{N}_{18}(\tau) < \bar{N}_{12}(\tau) < \bar{N}_6(\tau)$	0.162
190	41.5	$\bar{N}_{18}(\tau) < \bar{N}_{12}(\tau) < \bar{N}_{24}(\tau) < \bar{N}_6(\tau)$	0.752
205	44.8	$\bar{N}_6(\tau) < \bar{N}_{12}(\tau) < \bar{N}_{18}(\tau) < \bar{N}_{24}(\tau)$	<0.001
220	48.1	$\bar{N}_{18}(\tau) < \bar{N}_6(\tau) < \bar{N}_{12}(\tau) < \bar{N}_{24}(\tau)$	0.520
235	51.4	$\bar{N}_{18}(\tau) < \bar{N}_{24}(\tau) < \bar{N}_{12}(\tau) < \bar{N}_6(\tau)$	<0.05
250	54.7	$\bar{N}_{18}(\tau) < \bar{N}_{24}(\tau) < \bar{N}_6(\tau) < \bar{N}_{12}(\tau)$	<0.05
265	57.9	$\bar{N}_{24}(\tau) < \bar{N}_6(\tau) < \bar{N}_{18}(\tau) < \bar{N}_{12}(\tau)$	<0.001
280	61.2	$\bar{N}_6(\tau) < \bar{N}_{24}(\tau) < \bar{N}_{18}(\tau) < \bar{N}_{12}(\tau)$	<0.001
295	64.5	$\bar{N}_6(\tau) < \bar{N}_{12}(\tau) < \bar{N}_{24}(\tau) < \bar{N}_{18}(\tau)$	<0.05
310	67.8	$\bar{N}_6(\tau) < \bar{N}_{18}(\tau) < \bar{N}_{12}(\tau) < \bar{N}_{24}(\tau)$	<0.001

4.2.2 Predicting The Level of Postural Engagement

Once it was shown that $N(\tau)$ is indicative of the contexts of the task, it was investigated whether $N(\tau)$ could be predicted without any knowledge of the contexts of the task. The Mahalanobis distance classifier was used to predict which classification each observation $\mathbf{X}(\tau)$ belonged to.

In the first attempt, each observation was classified within the grouping $N(\tau) = [0, 1, 2, 3, 4, 5, \geq 6]$. Defining each observation as $\mathbf{X}(\tau) = [\mathbf{V}(\tau)]$ (i.e. defined as the ten posture variables at data point τ without any history of the measures), the cumulative postural engagement classification was predicted with estimated accuracy of 26.8%. The overall ability of the classifier to correctly predict classifications was greatly improved when posture variable histories were also used in defining each $\mathbf{X}(\tau)$. When observations were defined as $\mathbf{X}(\tau) = [\mathbf{V}(\tau), \mathbf{V}(\tau-16)]$, the estimated classification accuracy improved to 31.2%. When an even longer history of the posture variables was used to define the observations, $\mathbf{X}(\tau) = [\mathbf{V}(\tau), \mathbf{V}(\tau-16), \mathbf{V}(\tau-32)]$, estimated classification accuracy improved to 34.6%.

It has yet to be defined what resolution of $N(\tau)$ must be predicted to appropriately predict the contexts of the task. For instance, it may be found that predicting a high level versus a low level of cumulative postural engagement sufficiently infers the contexts of the task. Therefore, the same classification technique was used to classify $\mathbf{X}(\tau)$ within the groupings $N(\tau) = [\leq 2, \geq 3]$ and $N(\tau) = [\leq 1, 2-4, \geq 5]$. Again, each $\mathbf{X}(\tau)$ was defined both with and without the histories of the posture variables. Classifying observations within the grouping $N(\tau) = [\leq 2, \geq 3]$ was most accurate when $\mathbf{X}(\tau) = [\mathbf{V}(\tau), \mathbf{V}(\tau-16)]$ (estimated classification accuracy: 66.1%). Classifying observation within the grouping $N(\tau) = [\leq 1, 2-4, \geq 5]$ was most accurate when $\mathbf{X}(\tau) = [\mathbf{V}(\tau), \mathbf{V}(\tau-16), \mathbf{V}(\tau-32)]$ (estimated classification accuracy: 56.1%).

Compared to the probability of correctly predicting $N(\tau)$ by chance, the classifier most accurate at predicting the classification of the observations $\mathbf{X}(\tau) = [V(\tau), V(\tau-16), V(\tau-32)]$ within the grouping $N(\tau) = [\leq 1, 2-4, \geq 5]$. Using these criteria, $N(\tau)$ is predicted with an accuracy of 56.1%. This is 22.8% more accurate than predicting the classification by chance.

Table 6 summarizes classification of observations defined with and without posture variable histories within each of three groupings.

Table 6. Ability of the mahalanobis classification system to correctly predict $N(\tau)$

Classification Groupings	Observations Being Classified	Estimated Classifier Accuracy
$N(\tau) = [0, 1, 2, 3, 4, 5, \geq 6]$	$\mathbf{X}(\tau) = [V(\tau)]$	26.8%
	$\mathbf{X}(\tau) = [V(\tau), V(\tau-16)]$	31.2%
	$\mathbf{X}(\tau) = [V(\tau), V(\tau-16), V(\tau-32)]$	34.6%
$N(\tau) = [\leq 2, \geq 3]$	$\mathbf{X}(\tau) = [V(\tau)]$	65.3%
	$\mathbf{X}(\tau) = [V(\tau), V(\tau-16)]$	66.1%
	$\mathbf{X}(\tau) = [V(\tau), V(\tau-16), V(\tau-32)]$	65.1%
$N(\tau) = [\leq 1, 2-4, \geq 5]$	$\mathbf{X}(\tau) = [V(\tau)]$	49.5%
	$\mathbf{X}(\tau) = [V(\tau), V(\tau-16)]$	53.4%
	$\mathbf{X}(\tau) = [V(\tau), V(\tau-16), V(\tau-32)]$	56.1%

Appendix B shows how accurately each subset of a particular $N(\tau)$ grouping can be predicted with various observations. Typically, subsets that include higher levels of postural engagement are predicted more accurately than subsets with lower levels of postural engagement. Consider, for example, classifying observations defined as $\mathbf{X}(\tau) = [V(\tau), V(\tau-16),$

$V(\tau-32)$] into the grouping $N(\tau) = [\leq 2, \geq 3]$. Data points at which the known value of $N(\tau)$ is greater than or equal to 3 are correctly classified 86.5% of the time, but data points at which the known value of $N(\tau)$ is less than or equal to 2 are only correctly classified 43.8% of the time. Therefore, this means of predicting postural engagement is highly susceptible to indicating false positives (data points at which the known value of $N(\tau)$ is low but a high value is predicted) and highly unsusceptible to indicating false negatives (data points at which the known value of $N(\tau)$ is high but a low value is predicted). Appendix B also shows that the incidence of false positives increases when observations are defined with posture variable history, and the incidence of false negatives decreases. Although defining observations with posture variable histories improves overall classifier accuracy, it greatly decreases the ability to accurately predict low levels of postural of engagement.

4.2.3 Principal Component Analysis

Principal component analysis of the ten posture variables, $\mathbf{X}(\tau) = [V(\tau)]$, shows that the total variance described by these variables was to some degree redundant. Had the variables been completely independent, each of the principal components would account for an equal amount of the data's total variance; yet, this is not the case. Only the first four principal components account for at least 10.0% of the data's total variance, and cumulatively they account for 76.8% of the variance. Each of the first six principal components account for at least 5.0% of the data's total variance and collectively account for 90.3% of the variance. Principal components 7, 8, 9, and 10 each account for less than 5.0% of the data's total variance, and therefore it is questionable whether they simply represent random variability within the data.

However, plotting ‘Total Variance Accounted For’ versus ‘Principal Component’ shows that there is no clear point at which the variance accounted for drastically levels off (Figure 19). Therefore, there is not one distinct group of principal components accounting for the majority of the data’s variance and one distinct group accounting for random variability, which is often observed when analyzing principal components (Table 7).

Table 7. The variance accounted for by the principal components calculated from the ten posture variables, $V(\tau)$, over all 420 waves.

Principal Component	Total Variance Accounted For
1	34.1%
2	17.9%
3	13.5%
4	11.3%
5	7.6%
6	5.9%
7	3.5%
8	3.1%
9	2.0%
10	1.1%

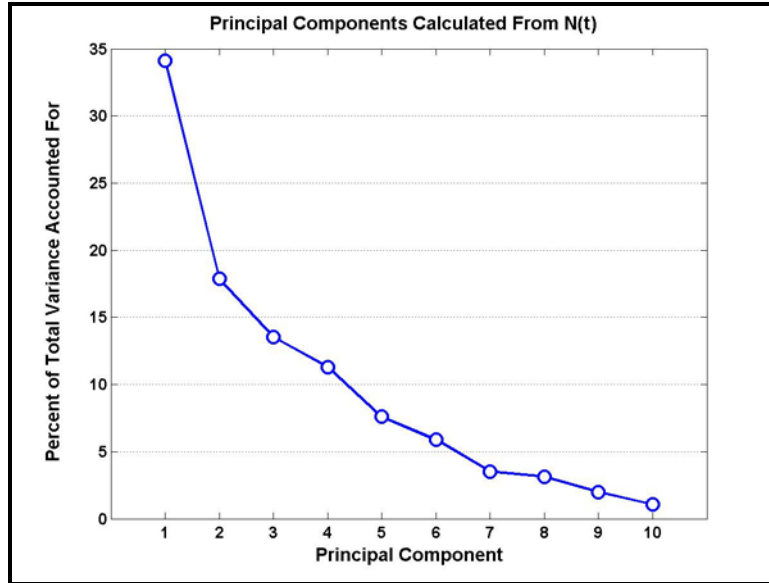


Figure 19. Principal components calculated from the observations $X(\tau) = [V(\tau)]$. Plotting the total variance accounted for by each principal component shows there is not a distinct group of principal components that appear to account for random variability.

Principal components were also calculated from the two sets of observations that were defined in part by posture variable histories, $X(\tau) = [V(\tau), V(\tau-16)]$ and $X(\tau) = [V(\tau), V(\tau-16), V(\tau-32)]$ (Figure 20, Figure 21). 13 of the 20 principal components calculated from $X(\tau) = [V(\tau), V(\tau-16)]$ and 25 of the 30 principal components calculated from $X(\tau) = [V(\tau), V(\tau-16), V(\tau-32)]$ account for less than 5.0% of the data's total variance. Plotting 'Total Variance Accounted For' versus 'Principal Component' shows that both sets of principal components have one distinct group of principal components accounting for the majority of the data's variance and one distinct group accounting for seemingly-random variability.

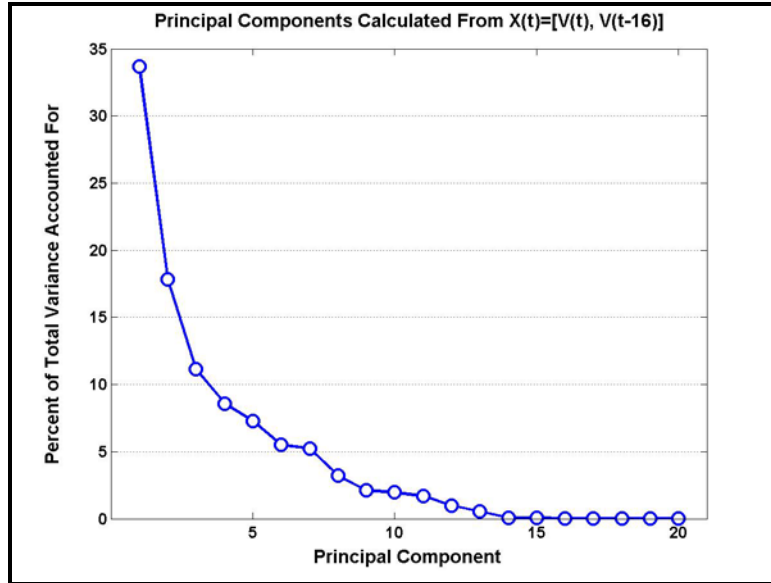


Figure 20. Principal components calculated from the observations $X(\tau) = [V(\tau), V(\tau-16)]$. The first 7 principal components each account for more than 5.0% of the total variance and collectively account for 89.3% of the total variance.

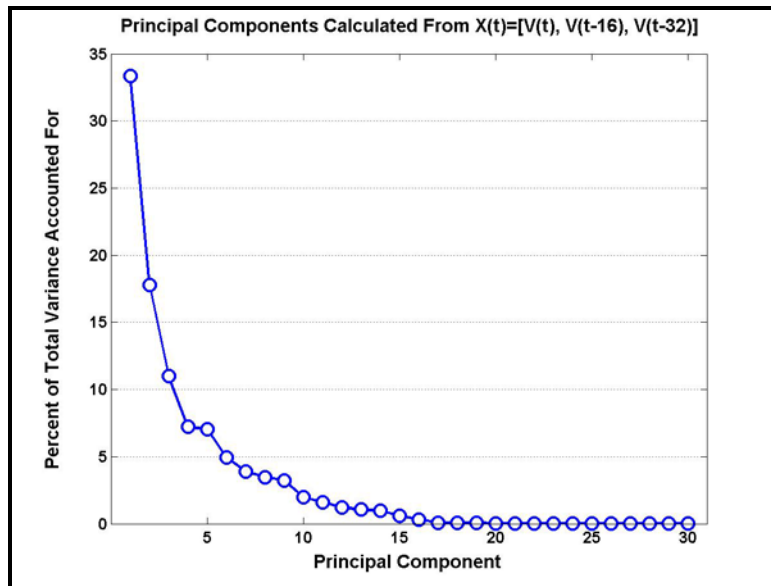


Figure 21. Principal components calculated from the observations $X(\tau) = [V(\tau), V(\tau-16), V(\tau-32)]$. The first 5 principal components each account for more than 5.0% of the total variance and collectively account for 76.4% of the total variance.

To determine if some principal components represented random variability that could be removed from the data, allowing $N(\tau)$ to be predicted with reduced dimensionality, the data was reclassified using principal component observations (opposed to posture variable observations). Three sets of principal components were calculated, one based on each of the observation sets defined in section 4.2.2: $X(\tau) = [V(\tau)]$; $X(\tau) = [V(\tau), V(\tau-16)]$; $X(\tau) = [V(\tau), V(\tau-16), V(\tau-32)]$. For each set of principal components, a new set of observations was defined by the principal components that account for at least 5.0% of the data's total variance. Again, each new set of observations was classified into the groupings $N(\tau) = [0, 1, 2, 3, 4, 5, \geq 6]$, $N(\tau) = [\leq 2, \geq 3]$, and $N(\tau) = [\leq 1, 2-4, \geq 5]$ (Table 8).

Table 8. Ability of the classifier to reproduce the correct classifications when the observations are defined posture variables in comparison to when they are defined by principal components that account for more that 5.0% of the data's total variance.

Classification Groupings	Posture Variables	Classifier Accuracy	
		Posture Variable Observations	Principal Component Observations
$N(\tau) = [0, 1, 2, 3, 4, 5, \geq 6]$	$X(\tau) = [V(\tau)]$	26.8%	24.0%
	$X(\tau) = [V(\tau), V(\tau-16)]$	31.2%	25.1%
	$X(\tau) = [V(\tau), V(\tau-16), V(\tau-32)]$	34.6%	21.9%
$N(\tau) = [\leq 2, \geq 3]$	$X(\tau) = [V(\tau)]$	65.3%	57.8%
	$X(\tau) = [V(\tau), V(\tau-16)]$	66.1%	58.5%
	$X(\tau) = [V(\tau), V(\tau-16), V(\tau-32)]$	65.1%	60.3%
$N(\tau) = [\leq 1, 2-4, \geq 5]$	$X(\tau) = [V(\tau)]$	49.5%	43.5%
	$X(\tau) = [V(\tau), V(\tau-16)]$	53.4%	44.7%
	$X(\tau) = [V(\tau), V(\tau-16), V(\tau-32)]$	56.1%	42.6%

Classifying the observations that are defined by principal components (with the low-variance components removed) is less accurate than classifying observations that are defined by the raw posture variables and their histories. The extent to which classifier accuracy is reduced ranges from a minimum of 2.8% and a maximum of 13.5%. In the case of classifying observations into the groupings $N(\tau) = [0, 1, 2, 3, 4, 5, \geq 6]$ and $N(\tau) = [\leq 1, 2-4, \geq 5]$, classifier accuracy is reduced the most when low-variance principal components are removed from the observations defined as $\mathbf{X}(\tau) = [V(\tau), V(\tau-16), V(\tau-32)]$. When classifying observations into the grouping $N(\tau) = [\leq 2, \geq 3]$, classifier accuracy is reduced the most when low-variance components are removed from the observations defined as $\mathbf{X}(\tau) = [V(\tau), V(\tau-16)]$.

5.0 DISCUSSION

5.1 GROSS POSTURAL CHANGES

ΔCOP , ΔBOS , and ΔSY were all significantly affected by the condition *wave type*. In general, subjects moved less as the maximum number of tracks on screen increased, and the difficulty of the air space monitoring task subsequently increased. There is no dynamic seated posture literature to compare these findings to, but these findings are similar to those reported in dynamic standing posture studies. Andersson et al [5] similarly reported that healthy young adults exhibit less postural sway while standing unperturbed and performing a mathematical task than while standing unperturbed with no second task (though the findings were not significant). The findings of the current study are also similar to those reported by Azevedo et al [9], who observed that subjects exhibited decreased standing postural sway in response to viewing disturbing images. These similarities do not imply that seated posture is characterized by some type of postural sway, but rather that increased arousal and stress may be associated with decreased postural dynamics, be it standing or seated posture.

It is important to note that there was an increase in postural movement, as demonstrated by all three measures of gross postural movement, during waves with 24 maximum tracks in comparison to waves with 18 maximum tracks (Figure 12, Figure 13, Figure 14). In each of the three measures, the increase was not significant and therefore might be attributed to random variance in the data. However, this increase in postural movement was accompanied by a

considerable degradation in task performance. From examining the ratio of wave score to the maximum possible score awarded in a wave, it is clear that performance suffers the most between *wave type*₁₈ waves and *wave type*₂₄ waves (Appendix A). It is possible that this increase in postural movement represents some change in the thought process that does not occur until a certain difficulty threshold is perceived. If this were true, one could predict that presenting subjects with more than 24 maximum tracks in a wave would continue to yield gross changes in seated posture greater than those reported in response to the *wave type*₁₈ waves.

It is important to consider whether the measured changes in seated posture are simply caused by motions that are required to perform the task, i.e. the arm and hand movements that are required to operate the computer mouse. Such asymmetric appendage movements change the position of the center of mass and subsequently the distribution of pressure over the seat surface. Yet, the three reported measures of gross postural change do not appear to be mere indicators of arm/hand movement. As the difficulty of the air space monitoring task increases, operators are required to identify and engage an increased number of tracks on screen. This in turn requires increased movement of the arm/hand to operate the computer mouse. However, subjects exhibited a decrease in gross seated postural changes as the number of tracks on screen increased. Thus, motions of the torso and/or head (e.g. leaning in the anterior/posterior direction) have a greater affect on these measures of changing posture than extremity movements that occur while operating the computer mouse.

The other wave conditions listed in Table 2 did not significantly affect ΔCOP , ΔBOS , or ΔSY . The fact that there was no interaction effect between *wave occurrence* and *wave type* nor *trial order* and *wave type* on gross postural changes implies that, within the scope of this experiment, subjects' posture did not change as they gained more experience performing the air

space monitoring task. It is possible that this would not be the case if seated posture changes were compared between novice and expert users. None of the subjects in the current study were considered expert users given their limited experience with the task. This lack of an interaction effect on gross postural changes also demonstrates the lack of any major fatigue effects within or between trials. If fatigue did affect posture in this experiment, one would expect to see a difference in gross postural changes between the first and third occurrence of similar *wave types* within a trial, or between similar *wave types* in separate trials. Again, these conclusions do not necessarily extend beyond the scope of this experiment, and an experiment could be designed differently to better investigate fatigue effects specifically.

Because gross postural changes are significantly affected by the maximum number of tracks on screen, it was concluded that these measures are significantly dependent on task difficulty. Therefore, one might expect to observe differences in gross postural changes between waves of different *trial type* (high versus low number of unidentified tracks). Although *trial type* significantly affected task performance scoring (Appendix A), neither affected gross postural changes. If the gross postural changes that have been reported are in fact dependent on task difficulty, then they are not sensitive to differences in task difficulty that result from the changing contexts of individual tracks. Instead, they are sensitive to broad changes in a task's global contexts, such as the total number of tracks on screen.

5.2 POSTURAL ENGAGEMENT RESPONSE

Demonstrating that gross postural changes are in some way dependent on task difficulty further justifies investigating the use of dynamic seated posture to gauge changes in cognitive state. These measures do not, however, provide a sense of how seated posture changes in response to changing task contexts in real-time due to their low temporal resolution. Real-time changes in seated posture were evaluated based on how the postural changes correlated to changing task conditions within a moving window. This notion of quantifying the degree to which seated postural changes mimic the changing number of tracks on screen was based on previous findings reported by Balaban et al [10], who showed that changes in anterior/posterior head position vary with workload at different points throughout the air space monitoring task. The cumulative postural engagement response that is reported in the current study captures a more wide-range of postural responses and allows us to quantify how closely posture mimics task conditions.

If we reexamine Figure 18 (average cumulative engagement response, \bar{N}), it is apparent that waves can be divided into an initial phase, middle phase, and end phase based on the posture-task relationship (Figure 22). The initial phase consists of the first 25 sec of a wave. During this phase, \bar{N}_6 , \bar{N}_{12} , \bar{N}_{18} , and \bar{N}_{24} are generally scaled according to their respective *wave type*, implying that \bar{N} is sensitive to the change in difficulty that accompanies increasing the total number of tracks on screen. Regardless of *wave type*, this phase is characterized by a peak in cumulative postural engagement response, which occurs while the number of tracks on screen is increasing. Physically, this response shows that the highly dynamic nature of the task (characterized by a high rate of track presentation) is accompanied highly dynamic changes in seated posture. It is during this time that tracks are being presented at a higher rate than the rate

at which subjects are identifying and attending to them. Because the task is not yet fully developed, operators are likely devoting substantial effort to redefining their global awareness of the wave conditions.

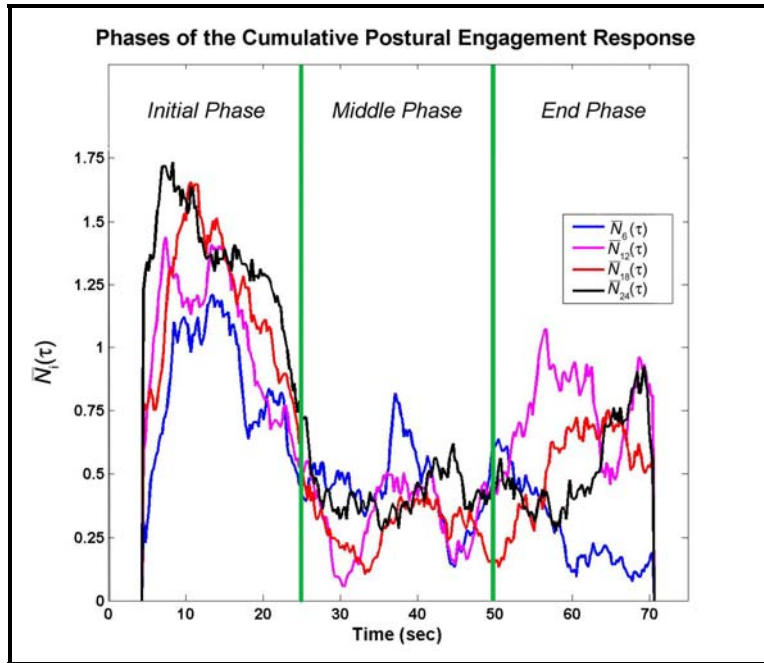


Figure 22. Segmenting the cumulative postural engagement response (\bar{N}). By examining \bar{N} calculated for waves with *wave type*₆, *wave type*₁₂, *wave type*₁₈, and *wave type*₂₄, waves can be segmented into an initial phase (0 to 25 sec), middle phase (25 to 50 sec), and end phase (50 to 75 sec).

The middle phase of the wave occurs between 25 and 50 sec. This phase is characterized by a relatively low \bar{N} , implying that subjects' changing postures cease to mimic the changing number of tracks on screen. In addition, \bar{N}_6 , \bar{N}_{12} , \bar{N}_{18} , and \bar{N}_{24} are not scaled in any consistent fashion, which implies that \bar{N} is not sensitive to task difficulty in the same manner that is was in the initial phase. As can be seen in Figure 17, the number of tracks on screen reaches its peak near the beginning of this phase, and so tracks are being identified and attended to at a higher

rate than the rate at which they are presented. This was not the case during the initial phase. Because the number of tracks presented to subjects is changing very little if at all during this phase, subjects are more likely to be updating their awareness of individual track conditions (local awareness) and less concerned with their awareness of the task as a whole (global awareness).

The end phase occurs during the final 25 sec of the wave. During the more difficult waves, subjects' changes in posture begin to mimic the changes in the number of tracks on screen again, as is apparent from \bar{N}_{12} , \bar{N}_{18} , and \bar{N}_{24} . In this final phase, tracks begin to leave the screen as the wave nears its end, even if they have not been identified. Like the initial phase, subjects likely devote much effort to redefining their global awareness of the task during this phase, because the less chaotic conditions make it very apparent that the wave is ending. In addition, subjects are still locally engaging individual tracks as they leave the screen and as the wave ends. Thus the end phase is accompanied by a sense of urgency that is not present during the initial phase.

The lack of postural engagement that was observed during the end phase of \bar{N}_6 is not consistent with the end phase observations of \bar{N}_{12} , \bar{N}_{18} , and \bar{N}_{24} . Unlike the more difficult waves, subjects were often able to identify and attend to all tracks on screen prior to *wave type₆* waves ending. As a result, often no change occurs in the number of tracks on screen during the end phase of *wave type₆* waves, and thus seated posture cannot be correlated to tracks on screen by definition. With the exception of \bar{N}_6 being visibly distinct from \bar{N}_{12} , \bar{N}_{18} , and \bar{N}_{24} , there does not appear to be any consistent scaling of the cumulative postural engagement responses as there was during the initial phase of the wave.

It is possible that the seated posture variables used to calculate N in the current study are simply measuring this same change in posture (e.g. anterior/posterior lean) in ten different ways. Principal component analysis of the ten posture variables (Table 3) shows us that there are six components of posture that account for non-random variance (components that account for more than 5% of the total variance). This implies that the ten posture variables collectively measure six independent postural adjustments. Therefore, there is redundancy in the variance accounted for by the ten variables, but surprisingly little. One might intuitively expect that only three distinct measures would actually exist, since subjects are essentially limited to rotating their torsos in the sagittal, frontal, and transverse planes. The identities of the six non-random postural adjustments are not yet clear based on the present analyses. However, it is clear that \bar{N} does not simply represent the correlation between the number of tracks on screen and ten different measures of the same postural adjustment.

The fact that $N(\tau)$ can be predicted with fairly high accuracy using a mathematical classification algorithm and without using any contexts of the task shows that certain postures are more likely to occur during different phases of the task. Table 6 shows that the ability to accurately predict $N(\tau)$ increases when the history of the posture variables are used to define the observation being classified at data point τ . Therefore, when an operator exhibits specific shifts in posture, he or she is likely to be posturally engaging the task. Based on the conclusions made above, we can further conclude that if the operator is moving in a certain way, then he or she is likely to be more focused on updating global awareness (beginning or end phase) or local awareness (middle phase).

$N(\tau)$ was also predicted by classifying principal component-defined observations, although prediction accuracy was greatly reduced (Table 8). The extent to which classifier

accuracy is reduced when low-variance principal components are removed implies that not all components that account for less than 5% of the data's total variance are measures of random variance. Appendix B shows that removing these components typically reduces the ability to accurately predict low postural engagement more than high postural engagement in comparison to those predictions made from posture-defined observations. Therefore, some low-variance principal components represent very small changes in posture that occur while subjects concentrate more on updating local situational awareness.

To summarize these findings, it appears that subjects' posture mimics task contexts more closely while the global contexts of the task are more dynamic (initial phase and end phase) and less closely while the global contexts of the task are more static (middle phase). Changes in seated posture therefore do appear to be dependent on changing contexts within a wave. In such a dynamic task, the maintenance of proper situational awareness can require a major effort from the operator, especially when the operator lacks substantial task experience [21]. Because updating awareness is cognitively demanding, it is concluded this means of classifying changes in seated posture is in fact a real-time cognitive state gauge.

While this gauge appears to be useful for detecting within-wave changes in task contexts, it does not appear to be able to detect between-wave changes. Although the values of $N(\tau)$ calculated for different *wave types* are significantly different, this gauge does not seem useful for discerning the actual number of tracks on screen in real-time. Therefore, calculating the cumulative postural engagement response in real time may be most useful as a means of detecting if operators cognitively engage a newly presented task or if they cognitively disengage from a task prematurely. Observing such reactions may help to conclude that the operator is not

cognitively prepared or lacks the cognitive capacity to attend to the task, and task presentation can then be adjusted appropriately.

5.3 SOURCE OF SEATED POSTURAL CHANGES

While the measures of gross postural changes and the real-time correlation between postural changes and task conditions reported in the current study help demonstrate that seated posture is dependent on task conditions, it is still not clear as to why these changes in posture occur. Previous work by Bull [15] implies that seated posture may be used to non-verbally convey intentions even while performing a task that does not require direct communication or interaction with any other people, such as the cognitive task performed in the current study. Although the gross changes in posture reported in the current study occur within a small range of motion, Pfungst [44] reports that humans do in fact convey information through very minute involuntary changes in posture that are difficult for other humans to detect. The subtle changes in posture that our subject population exhibited during this particular task would not be detected by the automated cognitive state detection system developed by Mota et al [41, 42].

Stoffregen et al [59] suggest that changes in posture serve a functional purpose, and somehow enable the individual to better perform the task at hand. For instance, in standing literature, a reduction in postural sway has been attributed to sharpening postural performance in order to reduce the threat of injury, which in turn enhances task performance [1, 5]. Although the postural threat hypothesis does not help explain the current study's findings since seated subjects are not faced with the threat of injury that standing subjects are faced with, it is still

possible that the changes in posture serve some other functional purpose. For instance, subjects may be positioning themselves so that they can more quickly operate the computer mouse.

As mentioned, many researchers have concluded that maintaining standing posture must involve some level of supraspinal (i.e. cognitive) input. It is possible that maintaining upright seated posture is similarly not as automatic as we tend to think it is. Even when seated subjects brace themselves against the back of the chair in order to reduce torso movement, they must still control motion of the head and the cervical and thoracic spine, which are not in contact with the back of the seat. If controlling these regions is cognitively demanding, then performing a second cognitive task may cause some change in seated postural control due to attention switching or limited cognitive resources.

Weeks et al [62] note that performing a cognitive task that requires motor system control (e.g. tracking tasks, reaction time tasks) may interfere with other motor tasks such as standing. If seated postural control does require some level of supraspinal input, then it also is susceptible to being interfered with by concurrently performed motor tasks. Since the cognitive task that was performed in the current study required computer mouse control, the changes in seated posture exhibited by subjects could also be the result of concurrent motor task performance. However, this hypothesis fails to explain the significance of the within and between wave changes in posture presented in the current study.

5.4 LIMITATIONS

All positional calculations (e.g. COP location) were based on the pressure sensors being spaced 1.0 in apart in a two-dimensional array. However, due to the deformable nature of the seat and back sensor mats, they are susceptible to creasing and folding, which can change the two-dimensional distances between sensors. Therefore, the accuracy and repeatability of such measures are potentially limited. This limitation can be addressed by developing a rigid pressure sensing mat, although this may prove to be uncomfortable for long-term sitting and subsequently inhibit the natural changes in seated posture reported in the current study.

Since no baseline data was collected, it is not clear to what extent seated posture varies during cognitive task performance in comparison to quiet sitting. Based on the trends in gross postural changes with respect to *wave type*, one might predict that a baseline condition would be characterized by greater gross postural changes than observed during *wave type₆* waves. However, if the gross postural changes that occur during difficult waves resemble the baseline posture, then it might be concluded subjects disengage from the task as it becomes more difficult.

As mentioned previously, performing a cognitive task that is dependent on subsequent motor tasks may interfere with postural control. To limit this potential effect subjects could be asked to perform a cognitive task that is not dependent on motor performance, such as a mental arithmetic task. Since we were mostly concerned with monitoring changes in posture in a realistic workstation scenario, using a purely mental was not a feasible alternative.

6.0 CONCLUSION

While performing a simulated air space monitoring task, subjects exhibited a decrease in total postural movement while tracking large waves of incoming aircraft than they did while tracking small waves of incoming aircraft. Based on these findings, it was concluded that alterations in dynamic seated posture are dependent on the contexts of a concurrently performed cognitive task. These findings are similar to those reported in standing posture literature, although it is not clear whether the functions of these standing and seated postural changes are similar.

The cognitive state gauge presented here is dependent on recognizing similarities between postural adjustments and changing task conditions. Throughout the course of the wave, postural changes were more highly correlated with the changing number of tracks on screen while the global conditions of the task were changing the most (i.e. the beginning and the end of the wave). Postural changes were poorly correlated with the changing number of tracks on screen while the global conditions were relatively constant (i.e. once the task was fully developed and few tracks were entering or leaving the screen). Knowing when subjects should be posturally engaging a task can be helpful in determining if they cognitively engage a newly presented task or if they cognitively disengage from a task ending prematurely.

All conclusions that were made in this study were based on observing the behavior of subjects while they encountered a realistic workstation scenario. It is therefore feasible to

conclude that monitoring changes in seated posture can be helpful in gauging the cognitive state of operators in real-life working environments. In addition, seated posture was successfully tracked completely unobtrusively. This means of gauging cognitive state would therefore allow seated operators to perform cognitive tasks in a natural and productive manner.

APPENDIX A

TASK SCORING

Table 9. Points Awarded for Identifying, Querying, Warning, and Firing on different types of tracks.

	Identify Track	Query Assumed Identity	Warn	Fire
Friendly	10	NA	0	0
Hostile	10	NA	0	75
Unknown (Assumed Friendly)	10	10	0	0
Unknown (Assumed Hostile)	10	10	10	50

Table 10. Maximum possible score for each wave within Trial J.

<i>Wave Number</i>	<i>Wave Type</i>	<i>Maximum Possible Score</i>
1	6	290
2	18	870
3	12	640
4	24	1220
5	6	290
6	18	930
7	12	580
8	24	1280
9	6	215
10	18	855
11	12	640
12	24	1280

Table 11. Maximum possible score for each wave within Trial K.

<i>Wave Number</i>	<i>Wave Type</i>	<i>Maximum Possible Score</i>
1	6	355
2	18	1065
3	12	635
4	24	1360
5	6	355
6	18	1065
7	12	710
8	24	1420
9	6	355
10	18	1065
11	12	660
12	24	1360

Table 12. Maximum possible score for each wave within Trial L.

<i>Wave Number</i>	<i>Wave Type</i>	<i>Maximum Possible Score</i>
1	6	290
2	18	930
3	12	640
4	24	1130
5	6	290
6	18	930
7	12	640
8	24	1280
9	6	215
10	18	930
11	12	640
12	24	1160

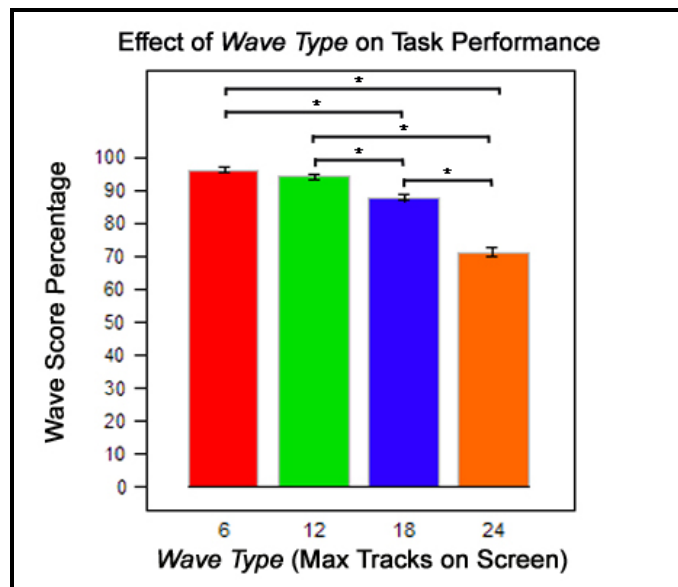


Figure 23. The average percentage of the maximum possible number of points awarded during different *wave types*. Standard error bars included.

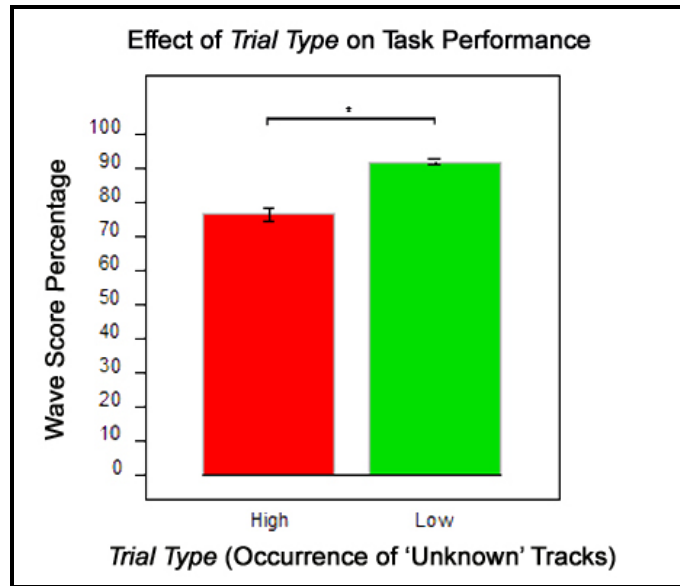


Figure 24. The average percentage of the maximum possible number of points awarded during different *trial types*. Standard error bars included.

APPENDIX B

CLASSIFIER ACCURACY

Table 13. Percentage breakdown of predicted $N(\tau)$ values for each subgroup of Known $N(\tau)$ Values ($N(\tau) = [0, 1, 2, 3, 4, 5, \geq 6]$, $\mathbf{X}(\tau) = [V(\tau)]$).

		Actual Classification of $N(\tau)$						
		0	1	2	3	4	5	≥ 6
Predicted Classification of $N(\tau)$	0	32.16	25.95	15.22	9.50	6.94	5.18	5.06
	1	12.22	17.50	15.13	9.78	7.41	1.73	3.80
	2	4.10	4.24	6.67	3.86	3.94	2.81	5.06
	3	12.40	13.63	20.90	35.78	26.92	20.09	16.46
	4	15.69	12.46	16.20	21.73	31.90	20.30	16.46
	5	15.48	16.00	15.83	10.87	12.10	38.23	27.85
	≥ 6	7.96	10.23	10.06	8.49	10.79	11.66	25.32

Table 14. Percentage breakdown of predicted $N(\tau)$ values for each subgroup of Known $N(\tau)$ Values ($N(\tau) = [0, 1, 2, 3, 4, 5, \geq 6]$, $\mathbf{X}(\tau) = [V(\tau), V(\tau-16)]$).

		Actual Classification of $N(\tau)$						
		0	1	2	3	4	5	≥ 6
Predicted Classification of $N(\tau)$	0	21.00	16.06	7.62	4.06	1.78	0.86	7.59
	1	19.32	23.14	15.22	8.45	7.32	3.67	5.06
	2	12.13	13.76	17.29	11.91	4.69	4.32	2.53
	3	10.08	11.03	17.35	31.67	19.51	12.74	0.00
	4	16.73	14.50	18.79	23.34	42.12	19.87	8.86
	5	20.73	21.47	23.73	20.52	24.48	57.67	50.63
	≥ 6	0.02	0.04	0.00	0.04	0.09	0.86	25.32

Table 15. Percentage breakdown of predicted $N(\tau)$ values for each subgroup of Known $N(\tau)$ Values ($N(\tau) = [0, 1, 2, 3, 4, 5, \geq 6]$, $\mathbf{X}(\tau) = [V(\tau), V(\tau-16), V(\tau-32)]$).

		Actual Classification of $N(\tau)$						
		0	1	2	3	4	5	≥ 6
Predicted Classification of $N(\tau)$	0	16.15	10.95	4.75	1.85	1.41	1.51	8.86
	1	23.74	27.78	16.20	8.73	7.32	6.05	5.06
	2	19.24	21.01	26.21	16.10	10.04	5.18	3.80
	3	16.55	17.59	25.83	47.28	27.77	15.34	3.80
	4	13.01	11.08	12.35	14.29	36.30	9.94	6.33
	5	11.31	11.60	14.67	11.71	17.17	61.56	45.57
	≥ 6	0.00	0.00	0.00	0.04	0.00	0.43	26.58

Table 16. Percentage breakdown of predicted $N(\tau)$ values for each subgroup of Known $N(\tau)$ Values ($N(\tau) = [\leq 2, \geq 3]$, $\mathbf{X}(\tau) = [V(\tau)]$).

		Actual Classification of $N(\tau)$	
		≤ 2	≥ 3
Predicted Classification of $N(\tau)$	≤ 2	58.66	28.02
	≥ 3	41.34	71.98

Table 17. Percentage breakdown of predicted $N(\tau)$ values for each subgroup of Known $N(\tau)$ Values ($N(\tau) = [\leq 2, \geq 3]$, $\mathbf{X}(\tau) = [V(\tau), V(\tau-16)]$).

		Actual Classification of $N(\tau)$	
		≤ 2	≥ 3
Predicted Classification of $N(\tau)$	≤ 2	50.33	18.03
	≥ 3	49.68	81.97

Table 18. Percentage breakdown of predicted $N(\tau)$ values for each subgroup of Known $N(\tau)$ Values ($N(\tau) = [\leq 2, \geq 3]$, $\mathbf{X}(\tau) = [V(\tau), V(\tau-16), V(\tau-32)]$).

		Actual Classification of $N(\tau)$	
		≤ 2	≥ 3
Predicted Classification of $N(\tau)$	≤ 2	43.78	13.51
	≥ 3	56.22	86.49

Table 19. Percentage breakdown of predicted $N(\tau)$ values for each subgroup of Known $N(\tau)$ Values ($N(\tau) = [\leq 1, 2-4, \geq 5]$, $\mathbf{X}(\tau) = [V(\tau)]$).

		Actual Classification of $N(\tau)$		
		≤ 1	2, 3, 4	≥ 5
Predicted Classification of $N(\tau)$	≤ 1	41.65	21.89	8.30
	2, 3, 4	30.01	50.62	35.42
	≥ 5	28.34	27.50	56.27

Table 20. Percentage breakdown of predicted $N(\tau)$ values for each subgroup of Known $N(\tau)$ Values ($N(\tau) = [\leq 1, 2-4, \geq 5]$, $X(\tau) = [V(\tau), V(\tau-16)]$).

		Actual Classification of $N(\tau)$		
		≤ 1	2, 3, 4	≥ 5
Predicted Classification of $N(\tau)$	≤ 1	35.18	12.86	4.61
	2, 3, 4	41.11	59.83	30.26
	≥ 5	23.71	27.30	65.13

Table 21. Percentage breakdown of predicted $N(\tau)$ values for each subgroup of Known $N(\tau)$ Values ($N(\tau) = [\leq 1, 2-4, \geq 5]$, $X(\tau) = [V(\tau), V(\tau-16), V(\tau-32)]$).

		Actual Classification of $N(\tau)$		
		≤ 1	2, 3, 4	≥ 5
Predicted Classification of $N(\tau)$	≤ 1	30.47	9.78	6.09
	2, 3, 4	56.33	74.15	30.26
	≥ 5	13.21	16.08	63.65

Table 22. Percentage breakdown of predicted $N(\tau)$ values for each subgroup of Known $N(\tau)$ Values ($N(\tau) = [0, 1, 2, 3, 4, 5, \geq 6]$, $X(\tau)$ = Principal Components derived from [$V(\tau)$] that account for more than 5% of the data's total variance).

		Actual Classification of $N(\tau)$						
		0	1	2	3	4	5	≥ 6
Predicted Classification of $N(\tau)$	0	15.39	11.97	8.06	7.93	4.97	5.83	1.27
	1	7.78	10.64	9.38	5.31	3.10	1.08	0.00
	2	10.53	10.06	12.35	7.24	8.91	10.80	10.13
	3	13.45	15.32	21.43	36.02	28.33	16.85	12.66
	4	31.65	29.24	26.04	26.84	36.30	29.59	16.46
	5	12.65	11.32	10.96	7.53	8.07	21.81	24.05
	≥ 6	8.54	11.45	11.77	9.13	10.32	14.04	35.44

Table 23. Percentage breakdown of predicted $N(\tau)$ values for each subgroup of Known $N(\tau)$ Values ($N(\tau) = [0, 1, 2, 3, 4, 5, \geq 6]$, $X(\tau)$ = Principal Components derived from [$V(\tau)$, $V(\tau-16)$] that account for more than 5% of the data's total variance).

		Actual Classification of $N(\tau)$						
		1	2	3	4	5	6	7
Predicted Classification of $N(\tau)$	0	14.99	10.99	6.58	6.40	5.53	5.83	0.00
	1	7.51	9.73	8.60	5.15	2.72	1.51	1.27
	2	14.10	14.49	15.20	11.11	11.16	11.66	8.86
	3	12.64	14.63	20.81	34.81	27.86	16.20	7.59
	4	29.70	28.40	25.44	25.84	36.59	23.54	18.99
	5	18.58	18.24	19.37	13.72	13.98	34.99	34.18
	≥ 6	2.49	3.53	4.01	2.98	2.16	6.26	29.11

Table 24. Percentage breakdown of predicted $N(\tau)$ values for each subgroup of Known $N(\tau)$ Values ($N(\tau) = [0, 1, 2, 3, 4, 5, \geq 6]$, $X(\tau)$ = Principal Components derived from [$V(\tau)$, $V(\tau-16)$, $V(\tau-32)$] that account for more than 5% of the data's total variance).

		Actual Classification of $N(\tau)$						
		0	1	2	3	4	5	≥ 6
Predicted Classification of $N(\tau)$	0	19.84	16.28	11.21	9.09	5.82	11.88	8.86
	1	5.71	9.01	8.48	4.39	2.06	0.00	0.00
	2	21.85	20.24	20.67	14.93	18.29	19.01	13.92
	3	17.09	19.05	24.14	40.16	32.65	22.03	16.46
	4	25.26	24.57	22.38	19.56	28.71	28.08	21.52
	5	2.68	2.52	2.48	3.82	3.19	5.83	10.13
	≥ 6	7.56	8.34	10.64	8.05	9.29	13.18	29.11

Table 25. Percentage breakdown of predicted $N(\tau)$ values for each subgroup of Known $N(\tau)$ Values ($N(\tau) = [\leq 2, \geq 3]$, $X(\tau)$ = Principal Components derived from [$V(\tau)$] that account for more than 5% of the data's total variance).

		Predicted Classification of $N(\tau)$	
		≤ 2	≥ 3
Predicted Classification of $N(\tau)$	≤ 2	35.41	19.72
	≥ 3	64.59	80.28

Table 26. Percentage breakdown of predicted $N(\tau)$ values for each subgroup of Known $N(\tau)$ Values ($N(\tau) = [\leq 2, \geq 3]$, $X(\tau)$ = Principal Components derived from [$V(\tau)$, $V(\tau-16)$] that account for more than 5% of the data's total variance).

		Predicted Classification of $N(\tau)$	
		≤ 2	≥ 3
Predicted Classification of $N(\tau)$	≤ 2	36.67	19.72
	≥ 3	63.33	80.28

Table 27. Percentage breakdown of predicted $N(\tau)$ values for each subgroup of Known $N(\tau)$ Values ($N(\tau) = [\leq 2, \geq 3]$, $X(\tau)$ = Principal Components derived from [$V(\tau)$, $V(\tau-16)$, $V(\tau-32)$] that account for more than 5% of the data's total variance).

		Predicted Classification of $N(\tau)$	
		≤ 2	≥ 3
Predicted Classification of $N(\tau)$	≤ 2	41.86	21.23
	≥ 3	58.14	78.77

Table 28. Percentage breakdown of predicted $N(\tau)$ values for each subgroup of Known $N(\tau)$ Values ($N(\tau) = [\leq 1, 2-4, \geq 4]$, $X(\tau)$ = Principal Components derived from [$V(\tau)$] that account for more than 5% of the data's total variance).

		Actual Classification of $N(\tau)$		
		≤ 1	2, 3, 4	≥ 5
Predicted Classification of $N(\tau)$	≤ 1	22.44	13.80	7.20
	2, 3, 4	39.61	49.96	34.69
	≥ 5	37.95	36.24	58.12

Table 29. Percentage breakdown of predicted $N(\tau)$ values for each subgroup of Known $N(\tau)$ Values ($N(\tau) = [\leq 1, 2-4, \geq 4]$, $X(\tau)$ = Principal Components derived from [$V(\tau), V(\tau-16)$] that account for more than 5% of the data's total variance).

		Actual Classification of $N(\tau)$		
		≤ 1	2, 3, 4	≥ 5
Predicted Classification of $N(\tau)$	≤ 1	21.27	11.67	7.38
	2, 3, 4	45.64	57.39	37.09
	≥ 5	33.10	30.94	55.54

Table 30. Percentage breakdown of predicted $N(\tau)$ values for each subgroup of Known $N(\tau)$ Values ($N(\tau) = [\leq 1, 2-4, \geq 4]$, $X(\tau)$ = Principal Components derived from [$V(\tau), V(\tau-16)$] that account for more than 5% of the data's total variance).

		Actual Classification of $N(\tau)$		
		≤ 1	2, 3, 4	≥ 5
Predicted Classification of $N(\tau)$	≤ 1	26.44	14.75	12.18
	2, 3, 4	50.83	62.53	49.08
	≥ 5	22.73	22.73	38.75

LITERATURE CITED

1. Adkin, A. L., J. S. Frank, M. G. Carpenter, and G. W. Peysar. "Postural Control Is Scaled to Level of Postural Threat." *Gait Posture* 12, no. 2 (2000): 87-93.
2. Al-Eisa, E., A. Fenety, D. Egan, and Crouse J. "Measurement of Sitting Pressure Distribution Under the Ischium: a Reliability Study." *Preceedings of the RESNA 2000 Annual Conference*. Winters J RESNA Press, 2000.
3. Alessandrini, M., G. D'Erme, E. Bruno, B. Napolitano, and A. Magrini. "Vestibular Compensation: Analysis of Postural Re-Arrangement As a Control Index for Unilateral Vestibular Deficit." *Neuroreport* 14, no. 7 (2003): 1075-9.
4. Amiridis, I. G., V. Hatzitaki, and F. Arabatzi. "Age-Induced Modifications of Static Postural Control in Humans." *Neurosci Lett* 350, no. 3 (2003): 137-40.
5. Andersson, G., J. Hagman, R. Talianzadeh, A. Svedberg, and H. C. Larsen. "Effect of Cognitive Load on Postural Control." *Brain Res Bull* 58, no. 1 (2002): 135-9.
6. Andersson, G. , J. Hagman, R. Talianzadeh, A. Svedberg, and H. C. Larsen. "Dual-Task Study of Cognitive and Postural Interference in Patients With Vestibular Disorders." *Otol Neurotol* 24, no. 2 (2003): 289-93.
7. Andersson, G., L. Yardley, and L. Luxon. "A Dual-Task Study of Interference Between Mental Activity and Control of Balance." *Am J Otol* 19, no. 5 (1998): 632-7.
8. Augmented Cognition International Society. "Advances Research Projects Agency ." Web page, [accessed 15 April 2006]. Available at <<http://www.augmentedcognition.org/>>.
9. Azevedo, T. M., E. Volchan, L. A. Imbiriba, E. C. Rodrigues, J. M. Oliveira, L. F. Oliveira, L. G. Lutterbach, and C. D. Vargas. "A Freezing-Like Posture to Pictures of Mutilation." *Psychophysiology* 42, no. 3 (2005): 255-60.
10. Balaban, C. D., J. Cohn, M. S. Redfern, J. Prinkey, R. Stripling, and M. Hoffer. "Control As a Probe for Cognitive State: Exploiting Human Information Processing." *International Journal of Human-Computer Interaction*. 17, no. 2 (2004): 275-86.
11. Bennett, B. C., M. F. Abel, and K. P. Granata. "Seated Postural Control in Adolescents With Idiopathic Scoliosis." *Spine* 29, no. 20 (2004): E449-54.

12. Berka, C., D. J. Levendowski, M. M. Cvetinovic, M. M. Petrovic , G. Davis, M. N. Lumicao, V. T. Zivkovic, M. V. Popovic, and R. Olmstead. "Real-Time Analysis of EEG Indexes of Alertness, Cognition, and Memory Acquired With a Wireless EEG Headset." *International Journal of Human-Computer Interaction* 17 , no. 2 (2004): 151-70.
13. Bloem, B. R., D. J. Beckley, B. J. van Hilten, and R. A. Roos. "Clinimetrics of Postural Instability in Parkinson's Disease." *J Neurol* 245, no. 10 (1998): 669-73.
14. Brauer, S. G., M. Woollacott, and A. Shumway-Cook. "The Interacting Effects of Cognitive Demand and Recovery of Postural Stability in Balance-Impaired Elderly Persons." *J Gerontol A Biol Sci Med Sci* 56, no. 8 (2001): M489-96.
15. Bull, P. E. *Posture and Gesture*, 3-13, 53-61, 98-107, 145-57. Oxford, England: Pergamon Press, 1987.
16. Carroll, S. "Situational Awareness Turning Data into Knowledge. (Operations)." *Journal of Electronic Defense*. 22, no. 9 (1999): 51-4.
17. Cassell, J., Y. I. Nakano, T. W. Bickmore, C. L. Sidner, and C. Rich. "Non-Verbal Cues for Discourse Structure." *Proceedings of the 39th Annual Meeting of the Association for Computational Linguistics*, 106-152001.
18. Cholewicki, J., G. K. Polzhofer, and A. Radebold. "Postural Control of Trunk During Unstable Sitting." *J Biomech* 33, no. 12 (2000): 1733-7.
19. Duncan, S., and D. W. Fiske. *Face-to-Face Interaction: Research, Methods, and Theory*, 3-12. Hillsdale, NJ: Lawrence Erlbaum Associates, 1977.
20. Duta, M., C. Alford, S. Wilson, and L. Tarassenko. "Neural Network Analysis of the Mastoid EEG for the Assessment of Vigilance." *International Journal of Human-Computer Interaction* 17, no. 2 (2004): 171-95.
21. Endsley, M. R. "Toward a Theory of Situation Awareness in Dynamic Systems." *Human Factors* 37, no. 1 (1995): 32-64.
22. Fenety, A., and J. M. Walker. "Short-Term Effects of Workstation Exercises on Musculoskeletal Discomfort and Postural Changes in Seated Video Display Unit Workers." *Phys Ther* 82, no. 6 (2002): 578-89.
23. Fenety, P. A., C. Putnam, and J. M. Walker. "In-Chair Movement: Validity, Reliability and Implications for Measuring Sitting Discomfort." *Appl Ergon* 31, no. 4 (2000): 383-93.
24. Flury, B., and H. Riedwyl. *Multivariate Statistics: a Practical Approach*, 181-233. Oxford, England: Chapman and Hall Ltd, 1988.

25. Force Sensitive Applications. "VERG, Vista Medical Ltd." Web page, [accessed 26 April 2006]. Available at <<http://www.pressuremapping.com>>.
26. Garner, K. T., and T. J. Assenmacher. "Improving Airborne Tactical Situational Awareness." *Journal of Electronic Defense* 19, no. 11 (1996): 42-6.
27. Geurts, A. C., T. W. Mulder, B. Nienhuis, and R. A. Rijken. "Dual-Task Assessment of Reorganization of Postural Control in Persons With Lower Limb Amputation." *Arch Phys Med Rehabil* 72, no. 13 (1991): 1059-64.
28. Hauer, K., M. Pfisterer, C. Weber, N. Wezler, M. Kliegel, and P. Oster. "Cognitive Impairment Decreases Postural Control During Dual Tasks in Geriatric Patients With a History of Severe Falls." *J Am Geriatr Soc* 51, no. 11 (2003): 1638-44.
29. Hermann, S. "Exploring Sitting Posture and Discomfort Using Nonlinear Analysis Methods." *IEEE Trans Inf Technol Biomed* 9, no. 3 (2005): 392-401.
30. Hickson, M. L., and D. W. Stacks. *Nonverbal Communication: Studies and Applications*, 87-119. Dubuque, IA: W.C. Brown Publishers, 1985.
31. Hooey, B. L., D. C. Foyle, and A. D. Andre. "Integration of Cockpit Displays for Surface Operations: the Final Stage of a Human-Centered Design Approach." *Proceedings of the AIAA/SAE World Aviation Congress*. Paper 2000-01-5521.
32. Hoover, A., and E. Muth. "A Real-Time Index of Vagal Activity." *International Journal of Human-Computer Interaction* 17, no. 2 (2004): 197-209.
33. Jahn, K., A. Deutschlander, T. Stephan, M. Strupp, M. Wiesmann, and T. Brandt. "Brain Activation Patterns During Imagined Stance and Locomotion in Functional Magnetic Resonance Imaging." *Neuroimage* 22, no. 4 (2004): 1722-31.
34. Kandel, E. R., J. H. Schwartz, and T. M. Jessell. *Principles of Neural Science: Fourth Edition*, 816-67. New York, NY: McGraw Hill, 2000.
35. Krzanowski, W. J. *Principles of Multivariate Analysis: a User's Perspective*, 223-35, 289-306. Oxford, England: Clarendon press, 1988.
36. Lajoie, Y., N. Teasdale, C. Bard, and M. Fleury. "Attentional Demands for Static and Dynamic Equilibrium." *Exp Brain Res* 97, no. 1 (1993): 139-44.
37. Maki, B. E., and W. E. McIlroy. "Influence of Arousal and Attention on the Control of Postural Sway." *J Vestib Res* 6, no. 1 (1996): 53-9.
38. Maki, B. E., A. Zecevic, H. Bateni, N. Kirshenbaum, and W. E. McIlroy. "Cognitive Demands of Executing Postural Reactions: Does Aging Impede Attention Switching?" *Neuroreport* 12, no. 16 (2001): 3583-7.

39. Marchese, R. , M. Bove, and G. Abbruzzese. "Effect of Cognitive and Motor Tasks on Postural Stability in Parkinson's Disease: a Posturographic Study." *Mov Disord* 18, no. 6 (2003): 652-8.
40. Melzer, I., N. Benjuya, and J. Kaplanski. "Age-Related Changes of Postural Control: Effect of Cognitive Tasks." *Gerontology* 47, no. 4 (2001): 189-94.
41. Mota, S. "Posture Analysis for Detecting Learner's Affective State." *Masters Thesis: Massachusetts Institute of Technology* (2002).
42. Mota, S., and R. Picard. "Automated Posture Analysis for Detecting Learner's Interest Level." *In Proc. CVPR Workshop on CVPR for HCI* (2003).
43. Norrie, R. G., B. E. Maki, W. R. Staines, and W. E. McIlroy. "The Time Course of Attention Shifts Following Perturbation of Upright Stance." *Exp Brain Res* 146, no. 3 (2002): 315-21.
44. Pfungst, O. *Clever Hanz (the Horse of Mr. Von Osten): a Contribution to Experimental Animal and Human Psychology*. New York, Hew York: Henry Hold and Company, 1911.
45. Prieto, T. E., J. B. Myklebust, and B. M. Myklebust. "Characterizing and Modeling of Postural Steadiness in the Elderly: a Review." *IEEE Transactions on Rehabilitation Engineering* 1, no. 1 (1993): 26-34.
46. Quant, S., A. L. Adkin, W. R. Staines, B. E. Maki, and W. E. McIlroy. "The Effect of a Concurrent Cognitive Task on Cortical Potentials Evoked by Unpredictable Balance Perturbations." *BMC Neurosci* 5 (2004): 18.
47. Quant, S., A. L. Adkin, W. R. Staines, and W. E. McIlroy. "Cortical Activation Following a Balance Disturbance." *Exp Brain Res* 155, no. 3 (2004): 393-400.
48. Redfern, M. S., M. L. Muller, J. R. Jennings, and J. M. Furman. "Attentional Dynamics in Postural Control During Perturbations in Young and Older Adults." *J Gerontol A Biol Sci Med Sci* 57, no. 8 (2002): 298-303.
49. Riley, M. A., A. A. Baker, J. M. Schmit, and E. Weaver. "Effects of Visual and Auditory Short-Term Memory Tasks on the Spatiotemporal Dynamics and Variability of Postural Sway." *J Mot Behav* 37, no. 4 (2005): 311-24.
50. Sala, S. D., and R. H. Logie. "Theoretical and Practical Implications of Dual-Task Performance in Alzheimer's Disease." *Brain* 124, no. Pt 8 (2001): 1479-81.
51. Schiffman, H. R. *Sensation and Perception: an Integrated Approach*, 202. New York, NY: John Wiley & Sons, Inc, 2001.
52. Schmorrow, D. , and D. McBride. "Introduction." *Journal of Human-Computer Interaction*. 17, no. 2 (2004): 127-30.

53. Shapiro, J. G. "Nonverbal Communication." *Sage Contemporary Social Science*, 61-6D. C. Speer. Beverly Hills, CA: Sage Publications, 1972.
54. Shin, Y. J., D. Gobert, S. H. Sung, E. J. Powers, and J. B. Park. "Application of Cross Time-Frequency Analysis to Postural Sway Behavior: the Effects of Aging and Visual Systems." *IEEE Trans Biomed Eng* 52, no. 5 (2005): 859-68.
55. Silfies, S. P., J. Cholewicki, and A. Radebold. "The Effects of Visual Input on Postural Control of the Lumbar Spine in Unstable Sitting." *Hum Mov Sci* 22, no. 3 (2003): 237-52.
56. Speer, N. K., K. M. Swallow, and J. M. Zacks. "Activation of Human Motion Processing Areas During Event Perception." *Cogn Affect Behav Neurosci* 3, no. 4 (2003): 335-45.
57. St. John, M., D. A. Kobus, J. G. Morrison, and D. Schmorrow. "Overview of the DARPA Augmented Cognition Technical Integration Experiment." *International Journal of Human-Computer Interaction* 17, no. 2 (2004): 131-49.
58. Stanney, K., S. Samman, L. Reeves, K. Hale, W. Buff, C. Bowers, B. Goldiez, D. Nicholson, and S. Lackey. "A Paradigm Shift in Interaction Computing: Deriving Multimodal Design Principles From Behavioral and Neurological Foundations." *International Journal of Human-Computer Interaction* 17, no. 2 (2004): 229-57.
59. Stoffregen, T. A., L. J. Smart, B. G. Bardy, and R. J. Pagulayan. "Postural Stabilization of Looking." *Journal of Experimental Psychology: Human Perception & Performance* 25, no. 6 (1999): 1641-58.
60. Tan, H. Z., L. A. Slivovsky, and A. Pentland. "Sensing Chair Using Pressure Distribution Sensors." *IEEE/ASME Transactions on Mechatronics* 17, no. 2 (2001).
61. Thomas, D. P., and R. J. Whitney. "Postural Movements During Normal Standing in Man." *J Anat* 93 (1959): 524-39.
62. Weeks, D. L., R. Forget, L. Mouchnino, D. Gravel, and D. Bourbonnais. "Interaction Between Attention Demanding Motor and Cognitive Tasks and Static Postural Stability." *Gerontology* 49, no. 4 (2003): 225-32.
63. Woollacott, M., and A. Shumway-Cook. "Attention and the Control of Posture and Gait: a Review of an Emerging Area of Research." *Gait Posture* 16, no. 1 (2002): 1-14.
64. Zacks, J. M., T. S. Braver, M. A. Sheridan, D. I. Donaldson, A. Z. Snyder, J. M. Ollinger, R. L. Buckner, and M. E. Raichle. "Human Brain Activity Time-Locked to Perceptual Event Boundaries." *Nat Neurosci* 4, no. 6 (2001): 651-5.
65. Zacks, J. M., B. Tversky, and G. Iyer. "Perceiving, Remembering, and Communicating Structure in Events." *J Exp Psychol Gen* 130, no. 1 (2001): 29-58.